

ENGINEERING OF FILAMENTOUS BACTERIOPHAGE  
FOR PROTEIN SENSING

by

MICHAEL BRASINO

B.A., University of Washington, 2011

M.S., University of California at San Diego, 2012

A thesis submitted to the  
Faculty of the Graduate School of the  
University of Colorado in partial fulfillment  
of the requirement for the degree of  
Doctor of Philosophy  
Materials Science & Engineering Program

2016

This thesis entitled:  
Engineering of Filamentous Bacteriophage  
for Protein Sensing  
written by Michael Brasino  
has been approved for the Materials Science & Engineering Program

---

Jennifer Cha

---

Joel Kaar

Date\_\_\_\_\_

The final copy of this thesis has been examined by the signatories, and we find that both the content and the form meet acceptable presentation standards of scholarly work in the above mentioned discipline.

Brasino, Michael David (P.D., Materials Science and Engineering Program)  
Engineering of Filamentous Bacteriophage for Protein Sensing

Thesis directed by Associate Professor Jennifer N. Cha

Methods of high throughput, sensitive and cost effective quantification of proteins enables personalized medicine by allowing healthcare professionals to better monitor patient condition and response to treatment. My doctoral research has attempted to advance these methods through the use of filamentous bacteriophage (phage). These bacterial viruses are particularly amenable to both genetic and chemical engineering and can be produced efficiently in large amounts. Here, I discuss several strategies for modifying phage for use in protein sensing assays. These include the expression of bio-orthogonal conjugation handles on the phage coat, the incorporation of specific recognition sequences within the phage genome, and the creation of antibody-phage conjugates via a photo-crosslinking non-canonical amino acid. The physical and chemical characterization of these engineered phage and the results of their use in modified protein sensing assays will be presented.

## **Dedication**

To Dani, for her patience with me and this work.

## Acknowledgments

Without my advisor Prof. Jennifer Cha, none of this work would be possible. Since Jen welcomed me into her lab at the University of San Diego, she has guided me through the twists and turns of my graduate studies, though it has by no means been a smooth journey. In between interviewing for her group and arriving to begin my graduate studies, my research interests shifted drastically from electronic materials to synthetic biology. Jen not only allowed me to switch to a new project but then allowed me to push that project into new directions outside the experience of the rest of the lab. She has continued to let me pursue my own research interests even when it has made it harder for her to advise me. I will always be thankful for the freedom this has given me in my work.

My graduate committee has given me support and encouragement throughout this work. On all occasions they have provided experienced advice and thoughtful criticism. I would like to specifically thank Prof. Joel Kaar for allowing me to use his laboratory for some of this work, for discussions concerning experimental design, and for his encouragement and interest in this research. Prof. Stephanie Bryant provided important guidance on the applications of this work while Prof. Dan Feldheim has offered me thoughtful advice concerning sensor design. Prof. Christopher Bowman not only supported this work by advising me as part of my committee, but by welcoming me into the Materials Science program at CU Boulder and guiding me through the newly formed program as one of its first students. I would also like to thank Prof Andrew Goodwin for his help in editing manuscripts produced from this work as well as for the use of his laboratory.

I would like to acknowledge the members of several labs at CU Boulder for their support as well. Current and past members of the Cha group have made a welcome, friendly and productive environment for this work to be done. This includes past members: Lauren Forbes, Hyunwoo Noh, Ju Hun Lee, Taeseok Oh, Matt Nakatsuka and Dylan Domaille. As well as current members: Ma Ke, Glenn Hafenstine, Liangcan He, Albert Harguindey Sanchez, Omer Yehezkeili, and Alex Harris. I have had the good fortune of working with two productive undergraduate students on this work; Mattias Greer and Andrew Frederickson. The Goodwin and Gill group members have also been particularly helpful by providing both material support and thoughtful discussion concerning this work. Several facility managers have also helped me in attaining data presented here. These include Annette Erbse, the director of the biochemistry instrumentation core; Jaime Kirshner, the director of the advanced sequencing core and Jeremy Balsbaugh, the director of the mass spectroscopy facility.

I would also like to thank everyone that has helped make the iGEM program possible at CU Boulder. My participation in this program has offered me inspiration and motivation throughout my graduate studies. The program would not be possible without its faculty advisor Prof. Robin Dowell or the funding provided by the Biofrontiers Institute and its associate director Jana Watson-Capps. Funding from Prof Larry Gold and Prof Marvin Caruthers also made the program possible.

My parents have supported me in all my endeavors, especially this one. My visits with them throughout my studies provided me with rejuvenating rest and relaxation. Their constant love and support has helped me through the times when this work was most trying.

## Contents

## Chapter

1. Introduction	
1.1. Review of historical bacteriophage research .....	1
1.2. Introduction to Filamentous Bacteriophage .....	2
1.3. Development of Filamentous Bacteriophage as a Research Tool .....	6
1.4. Filamentous Phage Based Biomaterials .....	11
1.5. Overview of the current work .....	14
2. Highly amplified ELISA signals from filamentous bacteriophage	
2.1. Introduction .....	16
2.2. Methods .....	18
2.3. Results and Discussion .....	21
2.4. Conclusion .....	30
3. Rolling circle amplification based sensing using bacteriophage	
3.1. Introduction .....	32
3.2. Methods .....	34
3.3. Results and Discussion .....	38
3.4. Conclusion .....	48
4. Antibody-phage conjugates as qPCR probes	
4.1. Introduction .....	50
4.2. Methods .....	52
4.3. Results and Discussion .....	55

4.4. Conclusion .....	67
Conclusions and future directions .....	68
Bibliography .....	71

## List of Tables

Table 2.1: Absorption peak intensities at 418 nm corresponding to sandwich ELISAs performed with Fzz8 phage previously conjugated with anti TNF detection antibodies. Capture antibodies at a concentration of 33 nM are absorbed onto polystyrene wells overnight at 4°C. Wells are blocked with BSA for 1 hr before adding the indicated concentration of TNF. TNF is detected with anti-TNF conjugated Fzz8 and antiM13-HRP.

Table 4.1: Sequence of primers used for Taqman probe based qPCR.

## List of Figures

Figure 1.1: Transmission electron micrograph of filamentous bacteriophage

Figure 1.2: Diagram of the filamentous phage structure

Figure 1.3: Depiction of a standard immunoassay used for the detection protein antigens.

Figure 2.1a: Schematic showing the use of dually modified phage for generating signal enhancement over antibodies alone.

Figure 2.1b. Schematic of the Fzz8 phage genome showing p3 coding sequence (orange), ZZ domain antibody binding fusion (red), p8 coding sequence (teal) and multiple cloning site (blue).

Figure 2.1c. SDS PAGE gel showing capsid proteins from M13KE control phage (left), Fzz8 phage (center), and a labeled protein ladder in kDa (right).

Figure 2.2a: MALDI-TOF spectrum of Fzz8 phage reacted first with 100 mM PLP and then different molar phage:alkoxyamine PEG biotin ratios

Figure 2.2b: MALDI-TOF spectrum of Fzz-AKT phage

Figure 2.3: Absorption spectrums surrounding the heme 403 nm peak of solutions containing 200 pMoles of HRP-avidin alone or with 2.6 pMoles of Fzz8 phage conjugated to biotin at a 1:2800 ratio and then passed through a .22 um filter.

Figure 2.4a: Polystyrene wells coated with 40 nM or 0 nM TNF $\alpha$  and incubated with biotin conjugated Fzz8 phage targeted with anti-TNF $\alpha$  antibody and detected with a HRP conjugated anti-M13 antibody. Absorbance readings for the 40 nM and 0 nM TNF $\alpha$  wells were 1.776 and .156 respectively.

Figure 2.4b: SPR sensorgram spectra comparing antibody-phage versus antibody alone. Association and dissociation curve of TNF $\alpha$  immobilized chip to anti-human TNF $\alpha$  antibody (top) and anti-human TNF $\alpha$  antibody conjugated Fzz8 phage (bottom). The insets show an expanded time-response curve at around 200 min.

Figure 2.5a: Average ELISA signals over background and standard deviations for 3 replicate assays with varying concentrations of rTNF $\alpha$  detected with Fzz8 phage reacted with 100 mM PLP and a 1:2800 molar excess of alkoxyamine, then conjugated with anti-rTNF $\alpha$  antibody.

Figure 2.5b: Bar graph of the data in 1.5A

Figure 3.1a: Rolling circle amplification products from the indicated phage concentration then digested with PstI endonuclease and run on an ethidium bromide stained agarose gel along with a DNA ladder. Largest DNA ladder band is 10 kilobases.

Figure 3.1b: Products quantified by fluorescence after mixing with SYBR green I dye.

Figure 3.2: Whole phage particles bearing 1 or 2 PstI recognition sites (1x or 2x) within their genome were mixed at the indicated ratio such that the total phage particle concentration was 339 pM and then amplified with RCA. Amplification products were digested with PstI endonuclease and ran on an ethidium bromide stained agarose gel.

Figure 3.3: Gel analysis of Figure 3.2 with ImageJ software showing fluorescence intensity moving down each gel lane.

Figure 3.4: Results of an assay for Rabbit IgG using phage expressing the antibody binding ZZ domain as RCA probes. Signals represent averages and standard deviations of four assays normalized to the no-target control in each assay. Amplification products are quantified by mixing with SYBR green 1 dye.

Figure 3.5: Results of an ELISA for Rabbit IgG using phage expressing the antibody binding ZZ domain as RCA probes. Since the absorbance values become very small below 3.33 pM target, similar signals are obtained at these low antigen concentrations.

Figure 3.6: (Top) Comparison of three ELISAs using peptide bearing phage at a concentration of 1.66 nM to probe varying concentrations of their respective targets. Results are listed by target.

Bound phage were detected with an anti-M13 HRP conjugate. (Bottom) Gel electrophoresis results using equal molar concentrations (~550 pM) of each phage type.

Figure 3.7: Fluorescence signals above background for RCA products created in the assay shown in Figure 3.8

Figure 3.8: (Top) Gel electrophoresis results of using an unequal mixture of the three phage sets to detect mixtures of targets at the indicated concentrations. The phage concentrations used were based on the relative affinities determined by phage ELISAs. The concentrations of the anti-lysozyme, anti-cMyc and anti-FLAG binding phage were at 1.66 nM, 166 pM and 1.66 pM respectively. (Bottom) imageJ analysis of gel shown. Peaks corresponding to bands created from phage products are indicated with arrows.

Figure 4.1: Phage were made to display on their p3 proteins two repeated Z domains containing the photo-crosslinking non-canonical amino acid pBPA on both (BPA-BPA) one (BPA-Z) or neither copy (Z-Z). A fourth phage was made to express only a single copy containing pBPA (BPA). a) Phage were irradiated with or without anti-TNF $\alpha$ , denatured and separated on a poly acrylamide gel shown. b) The same antibody-phage conjugates were tested for binding affinity to TNF $\alpha$  or additional anti-TNF $\alpha$  via ELISA using an anti-phage antibody conjugated with HRP.

Figure 4.2: Phage expressing only a single Z domain containing pBPA were mixed with anti-TNF $\alpha$  and irradiated for the number of hours listed. The resulting conjugates were denatured and separated on a poly acrylamide gel (a) or tested for binding affinity to additional anti-TNF $\alpha$  (b).

Figure 4.3: anti-TNF $\alpha$ -phage binding to TNF $\alpha$  after 3 hr, 6 hr and 14 hr photoirradiation: Phage irradiated for indicated amounts of time with anti-TNF $\alpha$  then used to detect various concentrations of TNF $\alpha$  immobilized on magnetic beads. Results show difference in ELISA signal over no TNF $\alpha$  control.

Figure 4.4: Gel electrophoresis based assay for detecting TNF $\alpha$ : anti-TNF $\alpha$ -phage were used to detect various concentrations of TNF $\alpha$  diluted in 0.1%PBST solution with 5 mg/ml BSA. Immunoassays were otherwise performed as reported in materials and methods. PCR was performed in a standard thermocycler for 25 cycles by adding assay beads directly to PCR reaction mixture containing primers, dNTPs and polymerase. After PCR reaction, reaction mixtures were added directly to a 0.75% agarose gels and electrophoresed for 30min at 120V. Samples are placed in the gel out of order to avoid any gel effects.

Figure 4.5: Validation of Taqman probes for real time PCR detection of phage in the presence of immunoassay magnetic beads: a) Indicated concentrations of phage are added to a real time PCR reaction mixture containing Taqman universal mastermix II (Life Technologies) along with phage specific primers (600 nM) and Taqman probe (250 nM) (Integrated DNA Technologies). b) Reactions were supplemented with 5  $\mu$ g of streptavidin functionalized magnetic beads (Dynabeads myONE streptavidin T1, Life Technologies).

Figure 4.6: Phage are conjugated with antibodies for the three targets listed and used to detect dilutions of said target in a sandwich type immunoassay using Taqman probe based qPCR for

signal quantification.  $\Delta C_t$  is the difference in threshold cycle for the listed concentration of target from a no-target control. Data points for each target represent the average and standard error of two independent assays.

Figure 4.7: Sequence specific real time PCR amplification of various phage via various primers: Taqman probe based real time amplification curves of the three phage types (Fz8b1,2,3) used for multiplex immunoassays diluted to  $1e9$  /ml in reactions with primer sets specific to each phage type (P1,2,3). In multiplex immunoassays, Fz8b1 was conjugated with  $TNF\alpha$ , Fz8b2 with IL6 and Fz8b3 with IL-1 $\beta$ .

Figure 4.8: Standard curves at low concentrations of three antigens in multiplex assay format: Each antigen listed is diluted to the indicated concentrations and tested in multiplex immunoassay format. Resulting  $\Delta C_t$  values for each dilution series are analyzed for lines of best fit through the least square method. Resulting logarithmic formula are used to calculate the indicated concentration from  $\Delta C_t$  values attained in later multiplex assays testing multiple antigens at once.

Figure 4.9: a) Standard curves for individual targets at various concentrations within a multiplex assay format using antibody-phage conjugates specific for each target. b) Multiplex assay results of various combinations of targets as calculated by the standard curves. Targets listed for each sample are at 10pg/ml. Results are the average and standard error of five independent assays.

## Chapter 1

### Introduction

#### Section 1.1: Early Bacteriophage Research

Bacteriophage meaning "bacteria eater" are viruses which prey on bacteria as their host. These diverse biological machines are ubiquitous in nature, where every strain of bacterium is predicted to have one or more bacteriophage that predate it.<sup>1</sup> But due to their size, it was not until the early 1900s that they were discovered. Since then, they have been crucial tools for our understanding of molecular biology as well as enabling a number of novel healthcare technologies. The first documented observation of bacteriophage was by Frederick Twort in 1915, who observed "glassy" and "transparent" areas when growing bacterial cultures. Twort further observed that these transparent growths could be transmitted from one colony to another through contact and that the agent causing the transparent growth passed through filters shown to remove bacteria.<sup>2</sup> However, Twort stopped short of concluding that this was due to a bacterial virus, instead stating that further study was needed. It was not until Felix d'Herelle independently observed bacteriophage growth in stool samples in 1917 and further characterized the phenomenon that the concept of bacteriophage became widespread.<sup>3</sup> Bacteriophage were immediately put to use as therapeutic agents by d'Herelle himself who observed that patients conditions improved upon administration of bacteriophage cultured from the disease causing bacterium.<sup>4</sup> Research in "phage therapy", as it came to be known, lessened with the development of penicillin, and has only recently been reinvigorated with rise of antibiotic resistance, but d'Herelle's discovery lead to the isolation of bacteriophage strains specific to many common bacteria.

These bacteriophage, in particular the phages of Escherichia Coli, enabled some of the seminal discoveries in molecular biology for decades after. So much so, that the scientists responsible for this work have come to be known collectively as the phage group. This includes Max Delbruck and Salvador Luria who in 1943 used the trait of phage resistance to demonstrate that bacteria accumulate genetic mutations similar to larger organisms.<sup>5</sup> Luria also used bacteriophage to discover genetic recombination and DNA repair in 1947 through dual infections.<sup>6</sup> The group expanded with Alfred Hershey and Martha Chase who in 1952 helped confirm DNA as opposed to protein to be genetic material by showing that phage mainly insert their DNA into host bacteria.<sup>7</sup> In 1950 Renato Dulbecco, who had studied phage under Luria and Delbruck used a similar procedure of phage plaque growth to grow and assay animal viruses plaques.<sup>8</sup> In the 50's multiple groups would observe the restriction of phage DNA within specific bacterial strains, leading to the discovery of restriction enzymes.<sup>1</sup> Seymour Benzer, after studying under Delbruck, would use the phenomenon of genetic recombination in phage to work out the first map of mutations within a gene, namely the T4 bacteriophage rII gene.<sup>1</sup> This bacteriophage gene would again be used by Francis Crick and others in 1961 to demonstrate the triplet nature of the genetic code.<sup>1</sup> The phage group primarily used a family of 7 different phage denoted T1-T7 for "type" in their work, because these strains underwent a straightforward lytic lifecycle and produced large plaques that were easy to view on a plate of E. Coli B cells.<sup>9</sup>

### **Section 1.2: Filamentous Bacteriophage**

As a tool for biotechnology, the strains used by the phage group were overly complex, having genomes well over 100 kilobases long. In 1963, a new type of bacteriophage of E. coli was isolated independently by Donald Marvin with Hartmut Hoffmann-Berling who called their

bacteriophage fd and Peter Hans Hofschneider who denoted it M13.<sup>10,11</sup> These bacteriophage came to be known as filamentous bacteriophage for their unique long capsid structure, and were later shown to be nearly identical to each other.<sup>12</sup> Compared to earlier bacteriophage, they were relatively simple, with a genome size of less than 7 kb and only 12 genes. Furthermore, they were unique in that they grew quickly and to high concentrations without greatly effecting the health or growth of their host *E. coli*. Because of this simplicity and facile production, these bacteriophage become a powerful tool for biotechnology. The most prominent example of this is phage display which I will discuss in detail.

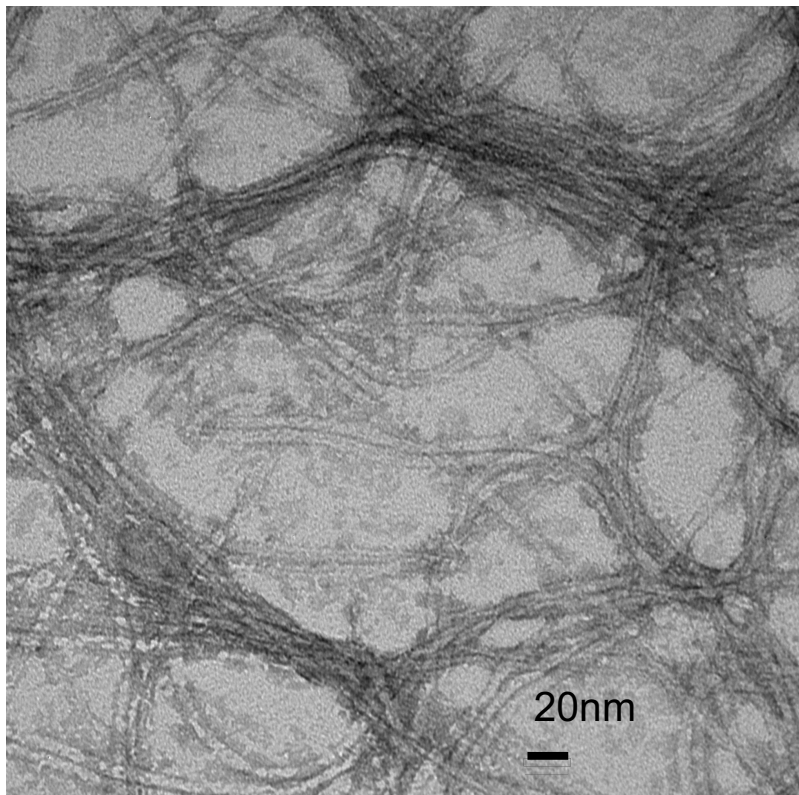


Figure 1.1: Transmission electron micrograph of filamentous bacteriophage

*Structure and Genetics of Filamentous Bacteriophage:* Filamentous Bacteriophage, specifically M13 and Fd which are the most studied, consist of an approximately 6408 bp circular single stranded DNA genome contained within a long protein capsid. The genome contains a total of eleven protein coding sequences which are transcribed from three promoters and are referred to as pI-pXI or sometimes p1-11 (as will be done here).<sup>13</sup> Five of these coding sequences are for capsid proteins which together form a filament approximately 6 nm in diameter and 900nm long. The most numerous protein in the filament is protein p8 (or p8), a 50 amino acid long alpha helical peptide which lines the side of the bacteriophage capsid with the C-terminal end interfacing with the genome in the center and the N-terminus pointing away. The p8 proteins spiral around the genome in a screw thread like pattern with their alpha helices pointed about 20 degrees toward the long axis. This forms a dull point at one end of the filament and an empty cone shape at the other. The other four capsid proteins are p3, p6 which are located at one end of the filament, and p7 and p9, which are located at the other. While there are approximately 2800 copies of p8 within each capsid, there are only 3 to 5 of each of these proteins. Of these, p3 is by far the largest, consisting of a 406 amino acid long chain containing three distinct domains linked by glycine rich regions and structured by internal cystein residues bridged with disulfide bonds.<sup>13</sup> These are the only cystein bridges within the capsid proteins.

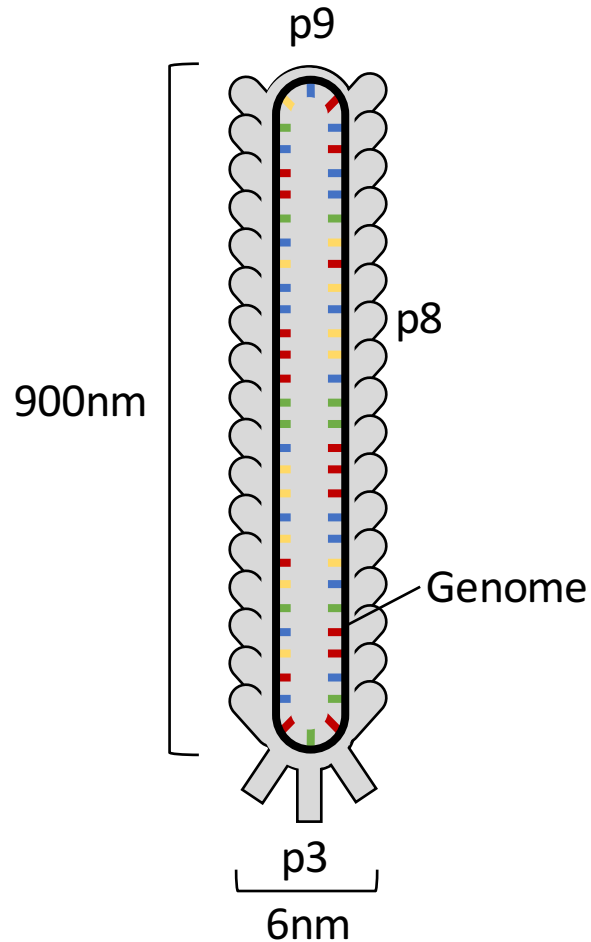


Figure 1.2: Diagram of the filamentous phage structure

*Filamentous Phage Life Cycle:* As mentioned above, the filamentous phage life cycle is part of what makes it unique among phage. Filamentous phage are only able to infect male E. coli, meaning strains that carry the F-episome and express an F-pilus for bacterial conjugation. At the start of the infection process, protein p3 binds to the f-pilus of male E. coli. The phage is then pulled into the E. coli cytoplasm where its coat proteins are removed and the phage genome is released. The phage genome is then replicated and, using a combination of phage and host cellular machinery, directs the production of additional phage coat proteins.<sup>13</sup> The phage coat

proteins are translated with signaling peptides at their N-terminus which direct them to the bacterial inner membrane such that the signal peptides sit within the periplasm where they are cleaved by proteases. The single stranded circular reverse complement of the phage genome is synthesized in excess and it is this DNA which is packaged into the new phage progeny (viral DNA). This occurs due to recognition of the phage packaging signal sequence on the viral DNA by phage proteins at the periplasm. The packaging signal, capped by coat proteins p7 and p9, is then extruded first through the bacterial membrane while being coated by p8 along its sides. Phage assembly is finished when all of the viral DNA is extruded at which point p6 and p3 cap the assembled capsid and are extruded last, releasing the new phage into the surrounding media.

### **Section 1.3: Development of Filamentous Bacteriophage as a Research Tool**

*Phage display:* Because of their simple structure and life cycle, filamentous phage were found to be ideal systems for the study of genetic regulatory systems. They were also found to be useful for the replication of large amounts of single stranded DNA.<sup>14</sup> However, their most common laboratory use today is for phage display. Phage display is the process of expressing peptides or proteins as fusions to phage coat proteins so that they are displayed on the exterior of the phage capsid.<sup>15</sup> This is done by inserting a nucleotide sequence coding for the peptide or protein into the coat protein sequence located on the phage genome. Filamentous phage proved remarkably tolerant of these modifications. George Smith originally demonstrated the concept of phage display by expressing 8 and 12 amino acid long peptides on the N-terminus of the p3 coat protein, which did not prevent the phage from growing to high concentrations within only a few hours.<sup>16</sup> Smith further showed that he could insert a mixture of randomized DNA sequences into the phage genome such that he would grow a mixture of phage, each expressing a random

peptide. He could then screen this mixture of phage (or phage library) for binding to other proteins (targets) by incubating a solution of the library over a surface on which the target is immobilized. By removing and washing away the library solution he could separate out only those phage that expressed peptides that bound to the target. He could then grow this select mixture of phage by adding them to a fresh culture of *E. coli* to create a new library enriched in phage expressing peptides that bound the target. Through multiple iterations of this process, which was termed "panning" in reference to the technique used to screen for gold, Smith could isolate peptides which mimicked the epitopes of several antibodies.<sup>17</sup> Phage display was enabled by the fact that each phage carried the sequence of the peptide it expressed, such that when the bound phage were amplified the peptides responsible for binding the target were amplified as well. Smith referred to this quality as the intimate link between phenotype and genotype.<sup>17</sup> This link was insured by always mixing the bound phage with an excess of *E. coli* during phage amplification which prevented any one bacterial cell from being infected by two types of phage at once, as this could allow phage to be produced with the genome replicated from one type and capsid proteins expressed from another.<sup>13</sup> As long as this was prevented, the sequence of the peptides that bound could be determined by sequencing the bound phage genomes. Often times, multiple rounds of panning would yield a mixture of phage bearing different peptide sequences, all of which contained a shorter consensus sequence with affinity for the target.<sup>17</sup> For example, one of the most widely reproduced phage display procedures has shown that the sequence histidine-proline-glutamine is found at some point in the peptide sequence when panning against the protein streptavidin.<sup>18</sup>

*Other phage display types:* The process of phage display was quickly expanded for the expression of larger amino acid sequences. This was enabled by the malleability of the

filamentous phage lifecycle. The problem with expressing larger sequences on protein p3 was that it interfered with the proteins function in phage infection. Smith was able to partially negate this effect by inserting a tetracycline resistance marker into the phage genome's origin of replication.<sup>16</sup> This did not abolish the phage genome replication but significantly slowed it down. Allowing more time for the expression of p3 proteins with larger fusions. It also allowed the infection of *E. coli* to be selected for via tetracycline. This prevented the *E. coli* from curing itself of the phage. Greg Winter's group in Cambridge used this strategy to produce the first phage expressing an antibody fragment on it's p3 coat protein.<sup>19</sup>

However, to express a library of these antibody fragments, the phage life cycle needed to be revised further. To do this, phage were produced expressing a mixture of both un-modified and antibody fragment linked p3 proteins through a phagemid-helper phage system.<sup>20</sup> In this system, a modified phage containing wild type capsid proteins but a disrupted packaging signal (helper phage) was infected into *E. coli* containing a plasmid bearing a un-disrupted packaging signal and an expression cassette for a modified p3 protein (phagemid). When both these constructs entered the cell, the helper phage expressed the wild type capsid proteins, including wild type p3 while the the phagemid expressed the modified p3. The phage produced had a mixture of both modified and un-modified p3 and contained phagemid DNA since this contained the non-disrupted packaging signal. As such. the phage produced still contained the information about the modified p3 that they were expressed with, which allowed them to bind targets and carry the information about what was binding. But at the same time, the phage still expressed some functional p3 on each particle which allowed them to still be infective. This allowed for the expression and screening of many different types of antibody fragments including single chain variable fragments (scFv) or even antigen binding fragments (Fab).<sup>20</sup> This offered an alternative

method of antibody engineering and affinity maturation to the costly process of immunization. It also allowed for the engineering of human type antibodies which could not be produced through immunization.<sup>21</sup> However, this process was not without its issues. It was observed that the vast majority of phage particles produced in this system carried no modified p3 at all, and the only particles that did carried only one.<sup>22</sup> These phage particles could still bind non specifically to targets or a substrate used in the panning process and enrich the pool of phage for the wrong modified p3. There was also a large percentage of phage produced which carried the helper phage genome instead of the phagemid. If these phage carried the modified p3, they could compete for binding to the target with correctly formed phage without carrying any information about their p3. Several groups have attempted to address these issues with various new helper phage or phagemids.<sup>22,23</sup>

Phage display was also adapted to use the other capsid proteins p8 and p9. Because of the relatively small size of p8, and the fact that so much of it is needed for phage growth, only small peptides which did not interfere with the p8 function could be expressed on all p8 proteins.<sup>17,24</sup> Larger peptides could be expressed by using an '88" type phage which contained both a wild type p8 and a separate synthetic p8 protein under an inducible promoter and fused with the peptide sequence.<sup>25,26</sup> This allowed the phage to assemble with the wild type phage while incorporating a smaller amount of modified p8. The advantages of this system over p3 display was that many more peptides were displayed per phage particle giving the phage a better chance of binding the target. It also allowed for the selection of peptides that might have lower affinity on their own but could work together at high valence to have higher avidity.<sup>24</sup> Display on p9 was developed later than other display schemes due to the fact that the p9 coding sequence overlaps with that of p7. Though proteins displayed on p9 could still be expressed from a separate phagemid, this

prevented the production of homogenous phage as discussed above.<sup>27,28</sup> This was circumvented by refactoring the phage genome such that p7 and p9 were made separate.<sup>29</sup> This allowed for the display of peptides without disrupting the infectivity of the phage.

*Diversification of panning targets:* As the location and types of amino acid sequences that could be expressed on phage expanded, the method of panning phage display libraries was also expanded for new targets. Smith originally used phage display to select phage capable of binding specific antibodies and phage display was soon used to find phage capable of binding a number of protein targets. With modifications to the standard panning process, traits other than binding affinity could also be selected for such as enzymatic activity.<sup>17,30</sup> Binding partners to protein targets could also be selected for in-vivo which allowed for the isolation of phage that became localized at specific organs or on specific cell lines.<sup>31</sup> This method was further expanded to allow for the selection of phage that could be endocytosed.<sup>32,33</sup> Non-protein targets such as small molecules or haptens could also be used in panning protocols, yielding phage which bound these targets as well.<sup>34-36</sup>

Particularly interesting to the field of material science has been the use of phage display to isolate peptides with affinity for specific materials surfaces. By panning a phage display (usually peptide) library against a specific material surface, peptides with affinity for that surface could be isolated. Using this method, peptides have been isolated with affinity for many different types of materials, including metals, ceramics, polymers and composites.<sup>37</sup> These peptides have been applied as either as molecular linkers, or as material synthesis agents.<sup>38</sup> As molecular linkers, these peptides can direct the assembly of proteins or materials into specific conformations. For example, material binding peptides can be fused to the end of proteins such as enzymes or antibodies to bind and orient them to either a patterned surface or nanoparticles.<sup>39,40</sup>

As materials synthesis agents, these peptides are used to control the nucleation or growth of specific materials or interfaces. A peptide isolated with affinity to a specific crystal face of a material can be used to modulate the shape of nanoparticles of that material by slowing the growth of that crystal face during synthesis.<sup>41,42</sup> However, a common pitfall of these peptides were their lack of specificity. Peptides isolated when panning a phage display library against one material such as gold were frequently found to bind to similar materials such as silver, sometimes with the same or increased affinity.<sup>43</sup> Though in one respect, this made these peptides more broadly applicable, the process of directing a peptide to one material and not the other remains challenging. This difficulty with specificity was partly helped by the use of negative screens in which the pool of phage found to bind the material of interest would then be screened for binding to a similar material, with the binders being discarded.<sup>38</sup>

#### **Section 1.4: Filamentous Phage Based Biomaterials**

The strategies for engineering filamentous bacteriophage that were developed for phage display also allowed for their use as a platform for biomaterials. This was done by taking the nucleic acid sequences found to bind in phage display to specific proteins or material targets and expressing combinations of them in various formats on the same phage. This took advantage of both the many different display formats already developed (p3, p8, 88, p9) and the convenience of keeping the targeting sequences in the same phage display system. The versatility of these phage scaffolds was also increased with chemical modification, either targeted to chemical groups accessible on wild type phage, or to specific modification handles introduced genetically. A large body of work has taken advantage of phage found to bind to specific targets in-vivo. For example, phage particles could be used as drug delivery materials by chemically conjugating

phage previously found to be bound or endocytosed in specific tissues with therapeutic compounds.<sup>29,44</sup> Similarly, these targeted phage could also be used as contrast agents for in-vivo imaging through the attachment of fluorescent or radiolabeled probes onto another part of the phage capsid either through the expression of peptides that bound the probe or through chemical conjugation.<sup>29,45-53</sup> Finally, the additional modification of the phage genome to carry transducing genes allowed phage to be used as gene delivery materials.<sup>54-58</sup> All of these in-vivo applications took advantage of the relatively low immune response phage illicit in mammals which allowed for increased circulation times.<sup>59</sup> However, it was imperative that phage used were sufficiently purified from bacterial debris present in the phage amplification culture and an adaptive immune response to the accessible portions of p8 protein has been documented.<sup>59,60</sup> Phage have also been used as scaffolds to create functional materials using the large number of material binding peptides discovered through phage display. This strategy has been particularly successful in the production of electronic materials. In a prime example, Yun Jung Lee et al. used a phage expressing peptides with affinity for single walled carbon nano tubes on p8 and amorphous iron phosphate on p3 to create a nanostructured lithium ion battery electrode.<sup>61</sup> In another example, Byung Yang Lee et al. working in Seung Wok Lee's lab was able to show that filamentous phage could be aligned within a thin film to form a piezoelectric material with properties modulated by a peptide sequence expressed on p8.<sup>62</sup> As such, filamentous phage not only provide a method of isolating ligands with desired properties through the process of phage display, but also form a convenient scaffold for expressing combinations of those ligands for a wide range of applications.

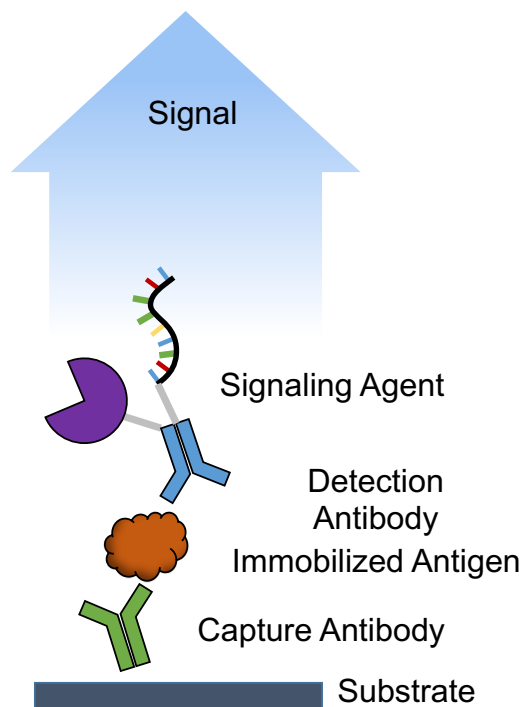


Figure 1.3: Depiction of a standard immunoassay used for the detection protein antigens.

*Phage Based Protein Sensors:* The current work concerns the application of phage based materials to the field of protein sensing. Past research in both the Cha lab and others has demonstrated the use of filamentous phage in this regard. In a standard immunoassay used for protein sensing depicted in Figure 1.3, the protein of interest within a biological sample is immobilized on a substrate either specifically, such as by binding an immobilized capture antibody (as shown), or non-specifically such as by direct absorption of the proteins within the sample to a surface. The immobilized protein of interest is then detected by adding a detection antibody specific for it. This detection antibody is either directly conjugated with a signaling agents such as an enzyme or is detected by a secondary antibody which is. Similar to the use of phage in other functional materials, this work leverages the ability to target phage to specific biomarkers via phage display. The presence of the protein of interest is then signaled either by

the presence of phage bound to the immobilized protein, or the presence of phage eluted from the protein after washing. The presence of phage in either case is detected via a number of different strategies. For example, previous work in the Cha Lab by Ju Hun Lee used phage expressing a peptide with affinity to anti-goat IgG as a replacement for a detection antibody in an immunoassay. The amount of immobilized anti-goat IgG was quantified by first adding phage, washing away unbound phage, and then eluting bound ones. Phage in the eluted solution were then quantified by the binding of gold nanoparticles either through DNA hybridization or thiol modification. The subsequent aggregation caused surface plasmon shifts in the gold nanoparticles which was easily detectable by a visible color change, the extent of which could be correlated to the amount of phage eluted and the concentration of antibody immobilized.<sup>63,64</sup> Eluted phage chemically conjugated with high concentrations of DNA could further be detected through the binding of surface enhanced raman spectroscopy active nanoparticles or through the binding of DNAzymes.<sup>65,66</sup> Because of the sequence specific nature of the DNA hybridization used in these studies, they showed potential for multiplexed protein sensing using a mixture of phage targeted to various proteins and each conjugated to a specific DNA sequence which could be identified via a DNA microarray. The present work sought to build off of these previous strategies while leveraging the ability to genetically engineer the filamentous bacteriophage.

### **Section 1.5: Overview of the Present Work**

In the present work, I have attempted to further explore the use of filamentous bacteriophage as a platform for protein sensing. I have done this by focusing on three elements of the bacteriophage structure. These are the major coat protein p8, the phage genome itself, and the phage minor coat protein p3. First I have attempted to engineer the phage coat protein p8 to

bind streptavidin conjugated HRP enzymes, which are commonly used in the protein sensing Enzyme Linked Immunosorbent Assays (ELISAs) for creating a signal. This way, by binding the phage to a specific protein target, the large number of p8 proteins exposed to the solvent on the sides of the phage would allow for many more HRP molecules to be bound per target than normally possible in ELISA. Second, I have explored methods of using the phage genome contained within each phage particle to signal both the presence and identity of the protein target to which a phage is bound. I have done this both through multiplexed rolling circle amplification as well as multiplex real time quantitative PCR. Finally, I will detail the development of a novel method for targeting phage to specific proteins through the display of an antibody binding peptide in which a photo-crosslinking non-canonical amino acid has been site specifically incorporated. I will review how this construct allowed for the creation of antibody-phage constructs capable of binding to specific antigens within a multiplexed sandwich immunoassay.

## Chapter 2

### Highly amplified ELISA signals from filamentous bacteriophage

#### Section 2.1: Introduction

In past years, extensive methods have been developed to both sense and identify different proteins in solution through enzymatic assays, in which a detection antibody binds to both an antigen and a signaling enzyme which produces a colorimetric signal.<sup>67-69</sup> A typical enzyme-linked immunosorbent assay (ELISA) requires three steps: first the antigen is sequestered to a surface or a surface-bound antibody, followed by the addition of a different antibody which binds the antigen as well as an enzyme capable of generating amplified signals, such as horseradish peroxidase (HRP). This enzyme then generates a colorimetric reaction by reacting with a substrate molecule.<sup>70</sup> Although ELISAs are now used routinely and extensively in medical facilities and laboratories, because the detection antibodies can only possess a finite number of attached enzymes (~1-4 HRPs per antibody), the signals generated for sensing are often limited to the nanomolar range<sup>71,72</sup>, especially in the case where the dissociation constant between antibody and antigen is high.<sup>70</sup> Though the binding strength of the antibody to an antigen can be limited, gains in sensitivity can be obtained by using a detection platform that possesses large surface areas for binding multiple enzymes, but still binds to a single antigen.<sup>73-75</sup>

In recent years, filamentous bacteriophage such as M13, Fd and their derivatives have been investigated as biological tools for materials science and biotechnology. The virus coat proteins may be genetically engineered to display different peptides and panning may be used to isolate unique binding motifs for a wide variety of substrates. Filamentous phage have been used as biosensors,<sup>63-66,76-79</sup> templating agents for energy relevant materials<sup>61,80,81</sup> and drug delivery

vehicles<sup>29,44,47,82,83</sup>. Of the five different proteins that comprise the filamentous phage capsid, two are commonly used as fusion partners to display peptides or small proteins. These are the 406-residue p3 proteins, which are present at three to five copies at one end of the virus, and the 50-residue p8 proteins, which are arranged in a helix around the length of the phage.<sup>13</sup> To enable the display of larger proteins on protein 3 such as antibody fragments that bind with greater specificity and affinity to antigens than short peptides, the genome of the Fd phage can be modified with a tetracycline resistance gene inserted into the origin of replication to create a modified phage known as Fd-tet.<sup>84,85</sup> In wild-type phage, protein fusions to p3 larger than about 20 amino acids typically prevent the p3 proteins from binding to the f-pilus of male bacteria and initiating the infection process, thereby preventing propagation. However, Fd-tet may be replicated without the need for infectivity because it can be maintained within a host culture through tetracycline selection. Because of this, Fd-tet phage have been used to clone libraries of large fusions such as antibody fragments<sup>86</sup> or IgG binding domains<sup>87</sup> onto the p3 proteins. Furthermore, the increased length of the Fd-tet genome causes the resulting phage to possess about 4000 p8 proteins as opposed to the typical 2700 p8 proteins seen in wild-type Fd.

For biosensing applications, the p3 proteins at the end of the phage are primarily responsible for binding a single antigen while the thousands of p8 proteins are modified to bind other materials. For example, in earlier work we showed that thiol groups or DNA strands could be attached to the viruses to bind metal nanoparticles to generate unique optical or spectroscopic signals.<sup>63,64</sup> In this study, we first show that genetically modified Fd-tet phage can bind the Fc portions of monoclonal antibodies and that these can be used to target specific antigens with high affinity and selectivity. Furthermore, we show methods to modify the p8 proteins with biotin groups without inhibiting the phage from binding to the detection antibody or the targeted

antigen. These biotin groups were then used to attach ~70 avidin conjugated HRP enzymes to each virus to yield large gains in signal in direct ELISAs over what can be achieved using antibodies alone (Figure 2.1a).

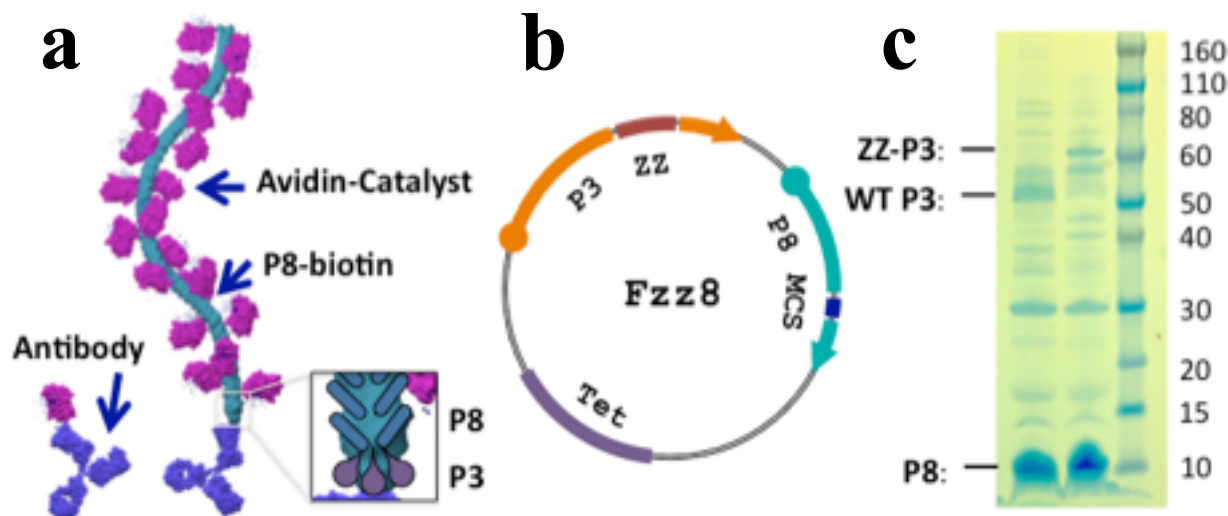


Figure 2.1: a. Schematic showing the use of dually modified phage for generating signal enhancement over antibodies alone. b. Schematic of the Fzz8 phage genome showing p3 coding sequence (orange), ZZ domain antibody binding fusion (red), p8 coding sequence (teal) and multiple cloning site (blue). c. SDS PAGE gel showing capsid proteins from M13KE control phage (left), Fzz8 phage (center), and a labeled protein ladder in kDa (right).

## Section 2.2: Methods

*Materials.* fUSE-5 genomic DNA was kindly provided by Prof. Itai Benhar. K91BlueKan cells were kindly provided by Prof. George P. Smith. Oligonucleotides were ordered from integrated DNA technologies. The highly competent Dh5 $\alpha$  cells, high fidelity polymerase, DpnI, BamHI, PstI and ligase enzymes were purchased from New England Biolabs. Miniprep kits were purchased from Quiagen. Gel extraction kits and 4-12% Bis-Tris SDS PAGE gels were

purchased from Life Technologies. Tetracycline hydrochloride, pyridoxal-5'-phosphate hydrate, bovine serum albumin, 2,2'-azino-bis(3-ethylbenzothiazoline-6-sulphonic acid) (ABTS) and Tween-20 were purchased from Sigma Aldrich. Alkoxyamine-PEG4-biotin and high binding polystyrene 96 well plates were purchased from Pierce Thermo Scientific. Recombinant human tumor necrosis factor alpha (rTNF $\alpha$ ), avidin conjugated horseradish peroxidase (HRP) biotinylated and un-modified versions of the anti tumor necrosis factor alpha antibody clone Mab11 were purchased from Affymetrix ebioscience. AntiM13-HRP antibodies were purchased from GE healthcare.

*Creating Fzz8 and Fzz8-AKT.* The fUSE-5 genome was modified with restriction sites for p8 cloning by site directed mutagenic PCR. Two rounds of mutagenic PCR were used to first remove the BamHI site located within the p3 coding sequence and then introduce a BamHI and PstI site at the N-terminus of p8. Each time the PCR products were digested with DpnI to remove template DNA, then transformed into Dh5 $\alpha$  cells and resulting colonies were screened for the correct mutation by digesting with the correct enzyme and analyzing on a .8% agarose gel. The resulting mutated fUSE-5 was named Fzz8 and was used to create Fzz8-AKT by cloning in the AKT sequence into the N-terminus of p8 via restriction ligation cloning. The Fzz8 genome was cut with BamHI and PstI and the larger fragment was purified by gel extraction. Oligonucleotides coding for the AKT sequence and compatible restriction sites were annealed together and then ligated into the Fzz8 fragment to re-circularize it as Fzz8-AKT. Phage were grown by transforming K91BlueKan cells with Fzz8 or Fzz8-AKT phage genomes and plating on LB plates with 40  $\mu$ g/ml tetracycline. Colonies were pricked from these plates and grown for 20-24 hrs at 37  $^{\circ}$ C with vigorous shaking in 80-160ml of LB with 40  $\mu$ g/ml tetracycline.

*PLP reaction and biotin conjugation.* Phage were reacted with pyridoxal-phosphate (PLP) by PEG precipitating a phage preparation and resuspending the pellet in freshly prepared 25 mM PBS pH6.5 at a concentration of about 141 nM. PLP was dissolved in the same buffer from frozen stock at a concentration of 200 mM by bringing the pH to approximately 6.5 with NaOH. 150 $\mu$ l of the phage and PLP solutions were mixed and reacted for 16 hrs at room temperature with mild shaking. Excess PLP was removed by PEG precipitating the phage four times. The resultant pellet was first re-suspended in 200 $\mu$ l of 10 mM PBS pH7.4, then in 1 ml of water twice, and finally in 200 $\mu$ l of water. PLP modified phage were diluted to a concentration of about 20 nM with 100 mM PBS pH4 prepared immediately beforehand and reacted with various concentrations of alkoxyamine-PEG4-biotin in the presence of 1 mM aniline.

*MALDI and SDS PAGE analysis.* MALDI-TOF spectrums were taken on a Voyager DE-STR system (ABI) after denaturing phage in a methanol, water, formic acid mixture and using tetrahydroxyacetophenone as a matrix. Phage were denatured for SDS PAGE analysis by dissolving in LDS (lithium dodecyl sulfate) loading buffer (Life Technologies) and heating at 80 °C for 10mins. PAGE gels were run for 35 mins at 200V and visualized by staining with Coomassie safe stain (Life Technologies).

*Surface Plasmon Resonance Studies.* BiOptix 404pi (Bioptix, U.S.A) and carboxymethyl dextran coated gold surface sensing chips (Bioptix, U.S.A) were used for the SPR assays. The protein coated gold chips were prepared by immobilizing human rTNF- $\alpha$  (PeproTech, Inc, U.S.A) to the dextran coated surfaces using carbodiimide chemistry. For this, 400 mM 1-Ethyl-3-(3-dimethylaminopropyl) carbodiimide (EDC) and 100 mM N-Hydroxysuccinimide (NHS) were injected simultaneously across the sensing spots for 5 min. Next, 3  $\mu$ g/mL rTNF $\alpha$  solutions in sodium acetate buffer (pH 4.5) were injected into all the channels. The surfaces were then

blocked with 1 M ethanolamine, pH 8.5 for 10 min. For determining binding constants, 5 nM anti human rTNF $\alpha$  antibody (eBioscience, U.S.A) or 5 nM anti human TNF- $\alpha$  antibody conjugated Fzz-phage in 0.05 % v/v PBST were injected into the experimental channels while 0.05 % v/v PBST was injected as control channels. The resulting spectra were analyzed by Scrubber 2 program (BioLogic Software, Australia).

*ELISA.* To target phage to rTNF $\alpha$ , 3 nM biotin conjugated Fzz8 phage were mixed at a 3:1 molar ratio with anti-rTNF $\alpha$  antibody clone Mab11 in 10 mM PBS pH 7.4. Unbound antibodies were removed by PEG precipitating the phage. Phage were re-suspended in blocking buffer (10 mg/ml BSA in 10 mM PBS pH7.4) at a concentration of 3.3 nM. The biotinylated version of the same targeting antibody (anti-TNF $\alpha$  antibody clone Mab11) was also made to be 3.3 nM in blocking buffer. rTNF $\alpha$  (ebioscience) was diluted in 10 mM PBS pH 6 and 50 $\mu$ l of each dilution was coated onto high binding capacity polystyrene wells for at least 16 hrs at 4 $^{\circ}$ C. The wells were then further blocked by adding blocking buffer and shaking at 170rpm for 1 hour at room temperature. 100  $\mu$ l of either the biotinylated antibody or phage solution was added to each well for 1.5 hrs. Wells were washed 3 times by pipetting in .01%PBST solution for 5 mins and tapping out gently on a paper towel. 100 $\mu$ l of avidin-HRP diluted in blocking buffer to the recommended concentration was added to each well for 1 hr and wells were washed as before. Signals from bound HRP were developed with ABTS for 10mins before removing solutions from wells and measuring the absorbance peak at 418 nm using a Beckman Coulter DU730 spectrophotometer.

### **Section 2.3: Results and Discussion**

In order to build highly sensitive protein sensors from filamentous bacteriophage, we chose to generate a virus that was capable of binding biologically relevant antigens via the p3 proteins located at the tip of the phage while conjugating multiple handles to the ~4000 p8 proteins to bind catalysts. For this, we first produced phage whose p3 proteins were genetically modified to display a repeated synthetic version of domain B from staphylococcus protein A (“ZZ” domain) that binds tightly with the Fc portion of IgG type antibodies.<sup>88</sup> The ZZ expressing phage (Fzz) could then be targeted to an antigen by conjugating it with an antibody specific to that antigen. For this, phage expressing two repeats of the IgG binding Z domain fused to each of the p3 coat proteins (fUSE5-ZZ phage) were first generously provided by Prof. Itai Benhar.<sup>87</sup> Next, in order to fuse specific peptides to each of the p8 proteins, the fUSE5-ZZ genome was further modified via site directed mutagenesis such that a BamHI and PstI site were located on either sides of the coding sequence for the N-terminus of the mature p8 protein (Figure 2.1b).<sup>84,89,90</sup> A BamHI site was also deleted within the p3 coding sequence such that the newly introduced restriction enzyme sites were unique. The introduction of the new BamHI site caused the third amino acid from the N-terminus of the mature p8 coat protein to change from aspartic acid to glutamic acid but all other mutations were silent. The new restriction enzyme sites would allow peptide sequences to be expressed as N-terminal fusions to all p8 coat proteins. The newly engineered genome termed Fzz8 was next transformed into chemically competent K91BlueKan cells and plated on LB plates containing 40 µg/ml tetracycline. Specific colonies were then grown overnight in K91BlueKan cells in LB with 40 µg/ml tetracycline at 37°C. After centrifuging the cells, the Fzz8 phage were precipitated out of solution by using 20 wt% PEG (MW 8000) and 2.5M NaCl. The resulting phage pellets were resuspended in 1 ml of 10 mM PBS pH 7.2, centrifuged for 5 mins to remove additional cell debris followed by a second PEG

precipitation step. The final phage concentration in solution was estimated by measuring the absorbance at 269 nm and 320 nm.<sup>13</sup>

To confirm the presence of the ZZ domain on the p3 proteins, SDS-PAGE gel electrophoresis was run. As a control, M13KE phage which carries a gene very similar to the wild type p3 protein was run as a negative control.<sup>91</sup> Both the Fzz8 and M13KE were first concentrated via a PEG precipitation and resuspended in water at a concentration around 1e14 particles per ml (166 nM) then denatured by mixing with lithium dodecyl sulfate (LDS) buffer (Life Technologies) and heating in a thermocycler at 80 °C for 10 minutes. As shown in Figure 2.1c, the Fzz8 lane clearly contains a band corresponding to a p3 protein conjugated with a ZZ domain while the M13KE lane contains only a band corresponding to the molecular weight of an unmodified p3 protein.

Next, in order to use the phage as detection platforms to produce highly enhanced ELISA signals, we decided to develop methods to conjugate multiple catalysts to each virus body. By doing so, we could increase the signal generated many fold for each antigen binding event over what can be achieved using antibodies alone which at most can only have a few enzymes attached. In order to achieve this, we decided to attach multiple biotin groups to the p8 proteins which could then be reacted with avidin-conjugated enzymes, such as horseradish peroxidase. While it is possible to detect the presence of phage by using an HRP conjugated anti-M13 antibody, this would require the need for an additional antibody which only increases the complexity and cost of the sensing assay. To chemically bind biotin groups to the p8 proteins, we employed a conjugation strategy developed by Francis and coworkers in which N-terminal amines are first converted to ketones by a transamination reaction with pyridoxal 5' phosphate (PLP) and are then reacted with alkoxyamine functionalized PEG4-biotin to form the

corresponding Schiff base.<sup>92</sup> By targeting only the N-termini of the coat proteins we minimized the chance of conjugating biotin groups to the p3 proteins and disrupting the phage binding to the targeting antibody. After reaction, the biotinylated Fzz8 phage was characterized by matrix assisted laser desorption ionization (MALDI) TOF mass spectrometry. As shown in Figure 2.2, the MALDI data contained two main peaks, one of which corresponded to the mass of the unmodified p8 coat protein (5253Da) while the other matched the expected molecular weight of a p8 protein fused to a PEG4-biotin group (5669Da). A smaller peak can also be seen in between these two which corresponds to the mass of the p8 protein modified with a PLP adduct. Higher amounts of biotin groups could also be attached per phage simply by increasing the amount of alkoxyamine PEG4-biotin added during the reaction (Figure 2.2a). However, as the number of PEG4-biotin groups per phage increased, this also caused the phage to become more difficult to precipitate out of the reaction mixture, thereby lowering the yields of biotinylated phage obtained. Using a molar ratio of 2800:1 alkoxyamine-PEG4-biotin to phage during the reactions produced biotinylated viruses that could easily be recovered from solution by PEG/NaCl precipitation. Next, to determine the number of enzymes that could be attached to each virus, 1 $\mu$ M avidin-HRP was added to 13 nM biotinylated Fzz8 in PBS and incubated at 4 °C for 1 hour. The solutions were then centrifuged through 0.22 $\mu$ m filters to determine how much of the HRP had bound to each phage by measuring the flow through by UV-Vis analysis. In order to make sure that the enzymes alone could pass through the filters, solutions of avidin-HRP were also filtered through 0.22 $\mu$ m filters. Through such measurements we were able to determine that approximately 70 avidin-HRP bound to each phage (Figure 2.3).

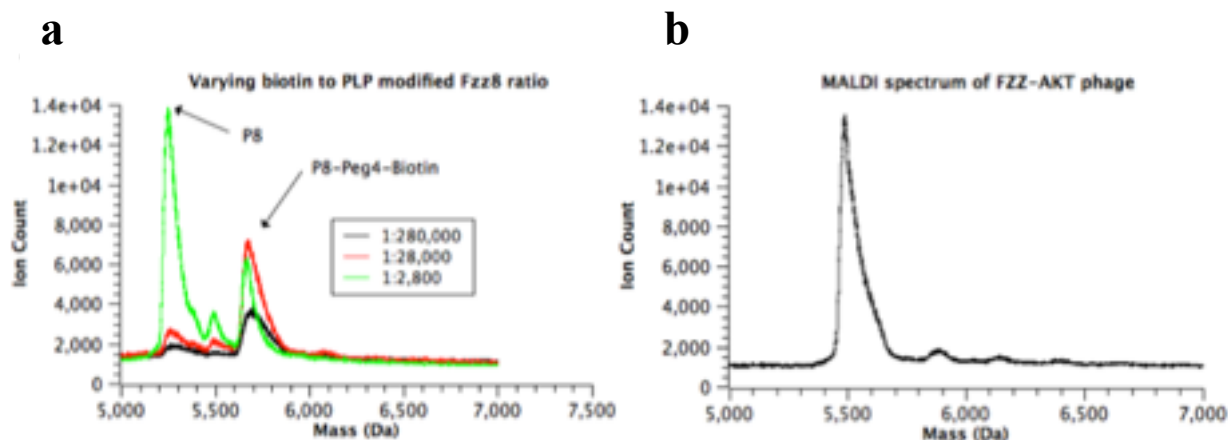


Figure 2.2: a: MALDI-TOF spectrum of Fzz8 phage reacted first with 100 mM PLP and then different molar phage:alkoxyamine PEG biotin ratios. b: MALDI-TOF spectrum of Fzz-AKT phage

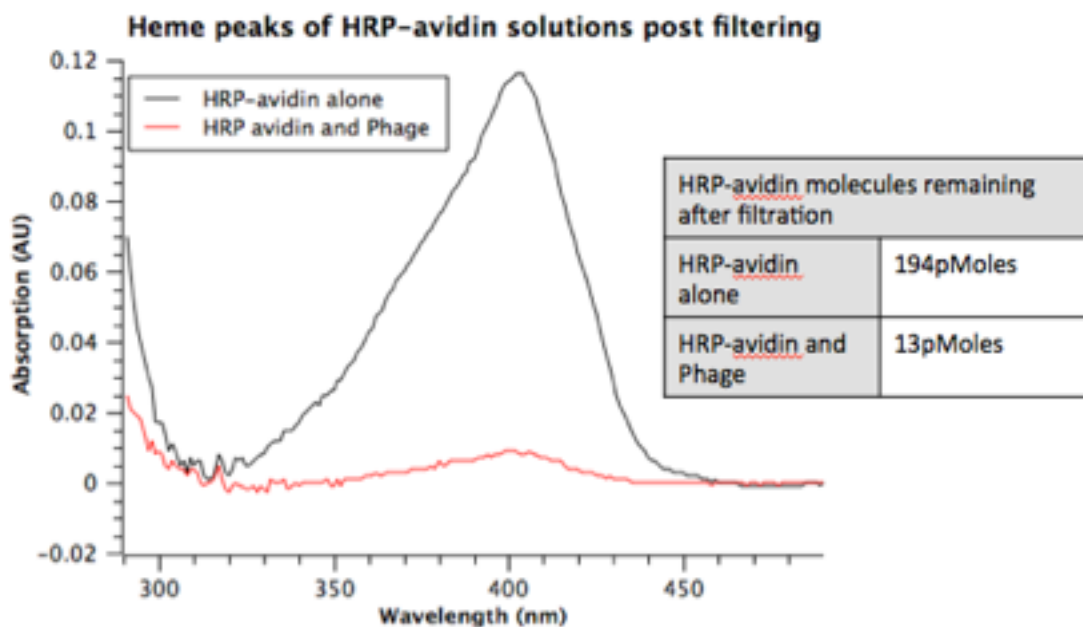


Figure 2.3: Absorption spectrums surrounding the heme 403 nm peak of solutions containing 200 pMoles of HRP-avidin alone or with 2.6 pMoles of Fzz8 phage conjugated to biotin at a 1:2800 ratio and then passed through a .22  $\mu$ m filter. The drop in heme concentration corresponds to a binding of 71.7 HRP-avidin-HRP molecules per phage particle added.

In addition to using Fzz8 phage that contain unmodified p8 proteins, the amino acid sequence alanine-lysine-threonine (AKT) was also genetically expressed at the N-terminus of the Fzz8 p8 proteins. The reason the AKT sequence was chosen was due to the observation that these peptides showed a higher oxidation rate of the N-terminus by PLP<sup>93,94</sup> which could further prevent any modification of the p3 proteins. For this, the lysine-threonine DNA sequence was inserted between the N-terminal alanine and the adjacent glutamic acid present in the wild-type protein. As shown in Figure 2.2b, MALDI analysis showed the expected molecular weight of a p8 protein fused to an additional lysine-threonine sequence (5669Da). However because the AKT expressing phage showed very limited solubility at neutral pH due presumably to the extra lysine group leading to an increased isoelectric point, we were unable to move forward in reacting the AKT modified viruses with PLP and alkoxyamine biotin.

To see if the Fzz8 phage could next be targeted to specific protein antigens, the biotinylated Fzz8 phage were conjugated with anti-recombinant human tumor necrosis alpha (rTNF $\alpha$ ) antibody by using a 1:3 molar ratio of phage to antibody in PBS for one hour at 4 °C followed by PEG precipitation. The resulting phage pellet was resuspended in 10 mM PBS pH 7.2 with 8.6 mg/ml BSA at a concentration of 3.3 nM. The antibody-conjugated phage were next reacted with high binding polystyrene wells bound with rTNF $\alpha$ . Any bound phage were reacted with HRP conjugated anti-M13 antibodies followed by thorough washing. ABTS and H<sub>2</sub>O<sub>2</sub> were then added to react with bound HRP. Control wells bound with no recombinant rTNF $\alpha$  and blocked with BSA were also tested simultaneously. As shown in Figure 2.4a, only the rTNF $\alpha$  bound well showed any colorimetric signal indicating that the Fzz8 phage could first successfully bind the anti-rTNF $\alpha$  antibody and second, that the antibody-conjugated phage could recognize the antigen rTNF $\alpha$ .

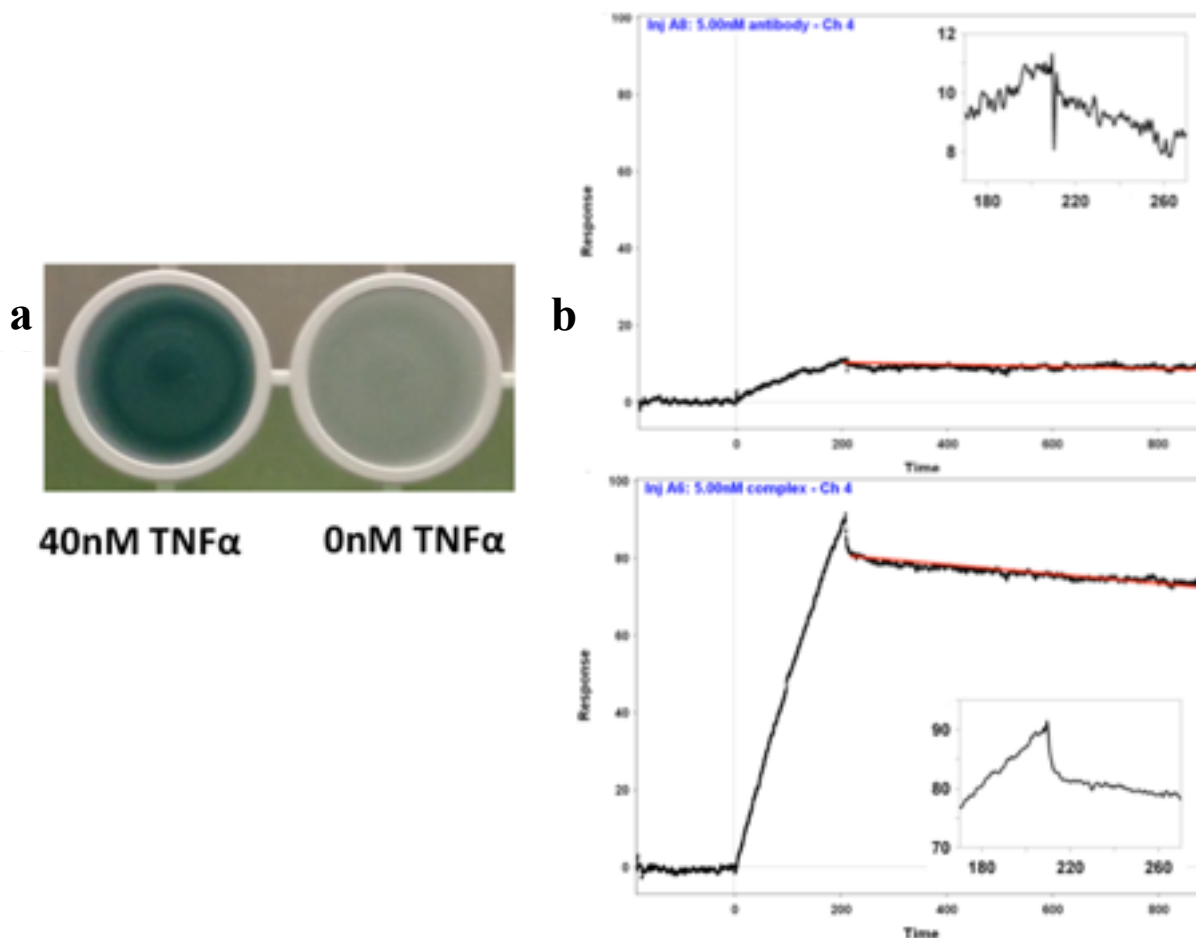


Figure 2.4: (a) Polystyrene wells coated with 40 nM or 0 nM TNF  $\alpha$  and incubated with biotin conjugated Fzz8 phage targeted with anti-TNF  $\alpha$  antibody and detected with a HRP conjugated anti-M13 antibody. Absorbance readings for the 40 nM and 0 nM TNF  $\alpha$  wells were 1.776 and .156 respectively. (b) SPR sensorgram spectra comparing antibody-phage versus antibody alone. Association and dissociation curve of TNF  $\alpha$  immobilized chip to anti-human TNF  $\alpha$  antibody (top) and anti-human TNF  $\alpha$  antibody conjugated Fzz8 phage (bottom). The insets show an expanded time-response curve at around 200 min.

In addition to using HRP conjugated anti-M13 antibodies for testing phage-antibody binding to the antigen, we also enlisted the use of surface plasmon resonance (SPR) to determine the dissociation constant ( $K_D$ ) values of phage-antibody versus antibody alone<sup>95-97</sup>. In the SPR assay, a carboxymethyl dextran coated gold surface was used to inhibit non-specific binding of

bacteriophage to the gold chip surface. Next, rTNF $\alpha$  was immobilized onto the dextran coated surfaces by carbodiimide chemistry. As shown in Figure 2.4b, the SPR sensorgram showed that even though antibody conjugated Fzz8 phage had a higher response unit (RU) due to having a mass 110 times that of the antibody, the  $K_D$  value of the complex to rTNF $\alpha$  was  $270 \pm 33$  pM (n=3), which was very close to the measured  $K_D$  value of the antibody alone ( $K_D = 298 \pm 99$  pM (n=3)). These results supported the continuing study of using phage-antibodies as biosensing platforms.

Capture Antibody + 19.6nM TNF	Capture Antibody + 0nM TNF	No capture Antibody + 0nM TNF
2.636	2.228	0.072

Table 2.1: Absorption peak intensities at 418 nm corresponding to sandwich ELISAs performed with Fzz8 phage previously conjugated with anti TNF detection antibodies. Capture antibodies at a concentration of 33 nM are absorbed onto polystyrene wells overnight at 4°C. Wells are blocked with BSA for 1 hr before adding the indicated concentration of TNF. TNF is detected with anti-TNF conjugated Fzz8 and AntiM13-HRP.

Next, to see if the biotin modified antibody-phage could enhance ELISA signals compared to biotinylated detection antibodies alone, we ran direct ELISAs using either reagent. A sandwich ELISA in which anti-TNF capture antibodies were immobilized to the polystyrene wells was also attempted but resulted in large background signals in the phage based assay (Table 2.1). This is likely due to the ZZ domain on the phage binding the immobilized capture antibody. In direct ELISA tests, the amount of antibody, avidin-HRP, ABTS and H<sub>2</sub>O<sub>2</sub> were kept constant between all wells while the concentration of rTNF $\alpha$  absorbed to the polystyrene wells was varied. First, 50 $\mu$ l solutions containing varying concentrations of rTNF $\alpha$  ranging from 40 nM to 0 nM in 10 mM PBS, pH 6 and BSA were absorbed for at least 16 hours to 96 well high-

binding polystyrene plates at 4°C. After removing the rTNF $\alpha$  solutions and washing, the wells were blocked further by adding 300 $\mu$ l of 10 mg/ml BSA in 10 mM PBS, pH7.2 and shaking gently at room temperature. After one hour, the blocking solutions were removed and 100 $\mu$ l of either the biotinylated phage-antibody or biotinylated antibody was added to each well for 1.5 hours, after which the wells were washed 3 times by adding 300 $\mu$ l of .01%PBST to each for 5 minutes. Next, 100 $\mu$ l of avidin-HRP (ebioscience) in 10 mg/ml BSA was added to react with any bound biotin groups for 1 hour followed by washing as above and the addition of 200 $\mu$ l of an ABTS/H<sub>2</sub>O<sub>2</sub> mixture in 50 mM citrate at pH4. After 10 minutes, the solutions were removed and the absorbance was measured at 418 nm. The average signals and standard deviations of 3 replicates of these assays are shown in Figure 2.5. The use of the biotinylated phage antibodies clearly showed a marked increase in ELISA signal over that using biotinylated antibodies alone. In these direct ELISA studies, as the concentration of TNF $\alpha$  decreased from 40 nM to 625 pM, the anti-rTNF $\alpha$  antibody based assay gave a limit of detection of 10 nM while the phage-antibody based assay showed a limit of detection at 2.5 nM. From this result it was observed that using phage-antibodies enabled a significantly lower detection limit than the antibody based ELISA. In order to increase the overall sensitivities of the assays, future studies will work both on using phage that genetically express the variable regions of antibodies as fusions to the p3 proteins.<sup>19,98,99</sup> Further gains in sensitivity may be achieved by expressing avidin binding peptides (histidine-proline-glutamine)<sup>24,100,101</sup> on the p8 proteins to alleviate the need for chemical conjugation which can not only in principle modify the p3 proteins but also requires purchasing alkoxyamine biotin compounds.

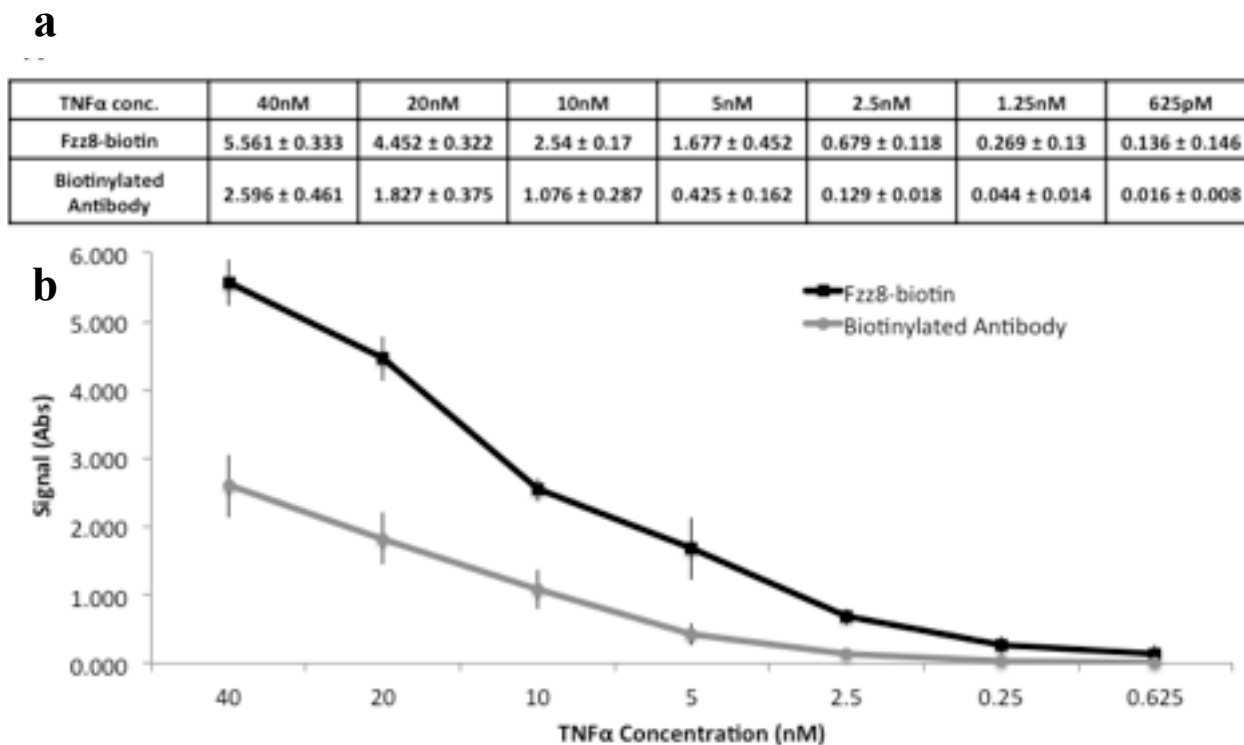


Figure 2.5: a: Average ELISA signals over background and standard deviations for 3 replicate assays with varying concentrations of rTNF $\alpha$  detected with Fzz8 phage reacted with 100 mM PLP and a 1:2800 molar excess of alkoxyamine, then conjugated with anti-rTNF $\alpha$  antibody. Signals are compared to assays done with a biotinylated version of the same antibody clone. b: Bar graph of the data in (a)

## Section 2.4: Conclusions

The early detection of disease has been shown to greatly increase the effectiveness of treatment and increase the overall health and wellbeing of patients. While ELISA is currently the most common method for detecting biomarkers, its limited detection sensitivity caused by insufficient and widely varying  $K_D$  values between antibodies and antigens has hindered its potential for sensing low antigen concentrations in biological media. In this work, we have empowered conventional ELISA techniques by engineering and using modified filamentous bacteriophage as sensing platforms. First, the phage were genetically engineered to bind to the Fc portion of detection antibodies, allowing them to bind specific antigens with higher specificity

than what can be achieved by using short peptide sequences. The genome of the viruses was also designed to enable cloning short peptide sequences onto the ~4000 p8 proteins. Next, multiple biotin groups were attached to the viruses by specifically modifying the N-termini of the coat proteins with ketone groups, which could then be reacted with alkoxyamine-modified biotin. The chemical modification of the coat proteins with biotin groups did not seem to prevent the p3 proteins from interacting with the detection antibodies. While previous research has shown that AKT sequences can increase the oxidation rate of the N-terminus by PLP, when all p8 proteins were modified with the AKT sequences, the phage became insoluble, hindering further use. Lastly, the biotinylated phage-antibodies were tested in direct ELISAs against antibodies alone to show that the phage-antibodies could yield on average 3 to 4-fold increase in signal at all antigen concentrations. Future work includes utilizing capture antibodies to improve antigen binding to surfaces as well as genetically expressing avidin binding peptides on the p8 proteins to avoid the need for chemical conjugation strategies.

## Chapter 3

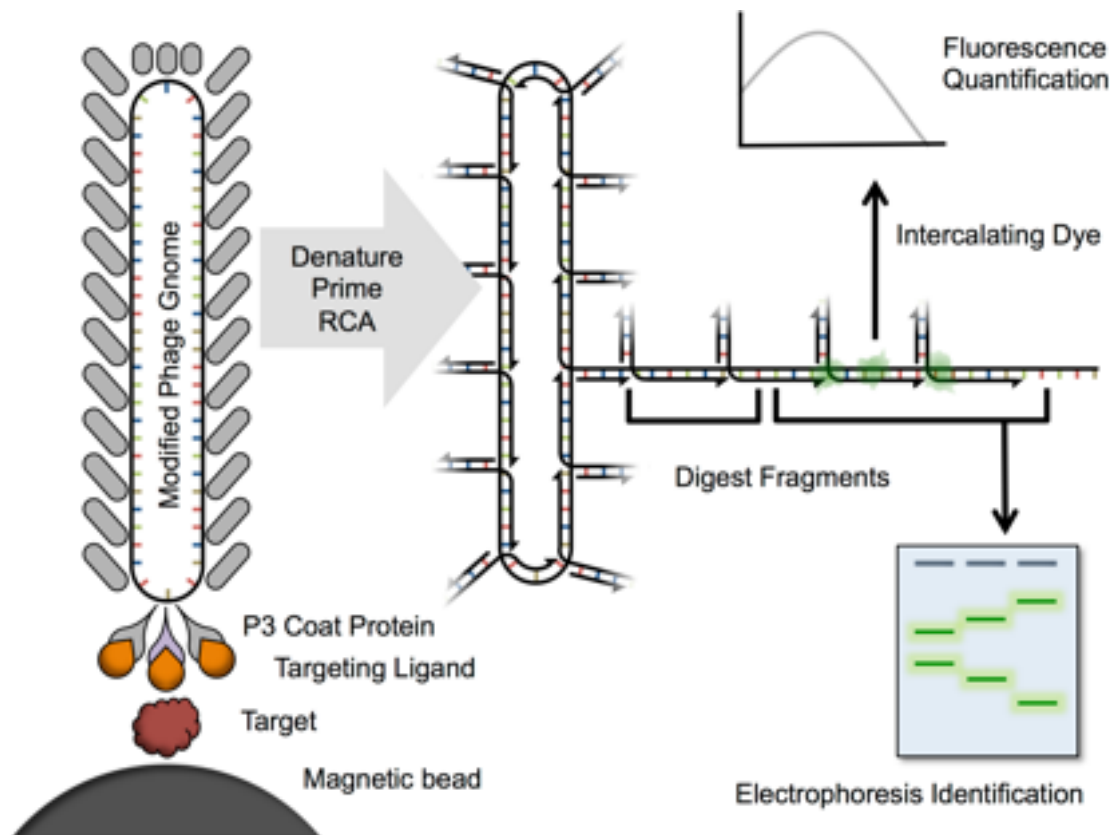
### Rolling circle amplification based sensing using bacteriophage

#### Section 3.1: Introduction

Since the introduction of immuno-PCR by Sano et al over two decades ago, there has been extensive research into the use of DNA amplification for detecting and quantifying specific proteins in solution.<sup>102</sup> These methods have typically relied on conjugating oligonucleotides to a targeting ligand such as an antibody. Because oligomers with various sequences can be attached to different antibodies and then amplified, this process can be used for multiplex analysis. However, these methods are significantly limited by the length and type of oligonucleotide that can be conjugated to a targeting moiety. It is difficult to attach long end-functionalized DNA strands to antibodies with any appreciable yields and the chemical methods used can also inhibit antibody affinities for specific antigens.<sup>103-105</sup> The need for short DNA strands also limits the number of variously sized templates that can be used in a single assay.<sup>106,107</sup> A more recent advancement has been the use of isothermal rolling circle amplification (RCA) as a way to create long concatemeric DNA strands that extend from primers attached to detection antibodies.<sup>108,109</sup> Known as immuno-RCA, this method utilizes small circular ssDNA molecules that anneal to primers attached to detection antibodies and are extended with a strand displacing polymerase. The advantage of this method is that the amplification products remain bound to the detection antibodies and can therefore be used in a microarray format for multiplexed sensing.<sup>109</sup> However, because the DNA attached to the detection antibody acts as a primer rather than a template, the amplification is linear rather than exponential. Furthermore, as the products are single stranded, their detection requires the use of either fluorescently labeled complementary oligomers or the

incorporation of fluorescent dNTPs, both of which increase the cost of the assay dramatically.<sup>108,109</sup>

Here, we demonstrate how genetically-engineered filamentous bacteriophage can be used as a multi-kilobase genome reporter for detection of specific protein analytes based on its ability to bind many types of targets and generate inexpensive, multiplexed signals through RCA amplification. First, filamentous phage are micron long viruses that infect bacteria and contain a circular single stranded multi-kilobase genome that codes for the coat proteins on the virus capsid. Filamentous bacteriophage were chosen as sensing platforms because peptides and recombinant antibody fragments that bind medically relevant targets can be isolated or expressed as fusions to their p3 and p8 coat proteins through phage display.<sup>13,19,24,47,64,66,76,77,79,84,92,110–112</sup> Recently, we also attached detection antibodies to phage by expressing an engineered IgG binding protein A fragment known as protein Z<sup>44,113</sup> as a fusion to the p3 proteins. Second, in this work the circular, single-stranded genome contained within the phage serves as a template for an RCA reaction. Unlike PCR, which has been used to detect phage before,<sup>114</sup> the RCA reaction rapidly and exponentially generates dsDNA in a single isothermal step, rather than multiple cycles. Furthermore, because the reaction generates dsDNA as opposed to ssDNA, the products can be easily detected using low-cost fluorescent nucleic acid stains. In addition, the large sequence of the viral DNA enables multiplexing without patterning or expensive fluorescent nucleic acid or DNA probes (Scheme 3.1). We demonstrate here that using the entire phage genome as an RCA template not only leads to high antigen detection sensitivities via a single isothermal reaction, but that the template can be applied to multiple simultaneous analyte sensing and typing by modifying multiple genomes with unique restriction enzyme sites (Scheme 3.1).



Scheme 3.1. Schematic depicting the use of phage and RCA of the phage genomes for antigen detection and typing.

### Section 3.2: Methods

*Rolling circle amplification of phage genomes from whole phage.* All solutions used in the reaction are first placed in eppendorf tubes and irradiated in an aluminum foil lined box approximately 15 cm below an 8 watt 254 nm UV lamp for 15 mins. Phage particles are diluted to the desired concentration in 5 ul of HPLC grade water in irradiated PCR tubes. Degenerate thio-phosphate linked RNA hexamer primers are diluted to 40 uM in annealing buffer (60 mM Tris-HCl pH7.5, 40 mM KCl, 16 mM MgCl<sub>2</sub>) and 5 ul is added to each PCR tube. Tubes are heated to 95 °C for 1 min and then allowed to cool to room temperature by leaving on the lab bench for 25 mins. dNTPs and polymerase are combined along with buffer to make a 2X RCA

reaction mixture (40 mM Tris-HCl pH7.5, 80 mM KCl, 9 mM MgCl<sub>2</sub>, 20 mM (NH<sub>4</sub>)<sub>2</sub>SO<sub>4</sub>, 8 mM DTT, 1 mM each dNTP (New England Biolabs), 5U(5 ng/ul) phi29 polymerase (Replipi Epicentre)) before adding 10ul to each PCR tube, vortexing briefly, and incubating tubes at 30 °C for 2 hrs. Reactions stopped by heating tubes to 65 °C for 10mins to denature polymerase.

RCA products were quantified by diluting the 20ul reaction volume to 200ul with TAE buffer (50 mM Tris-acetate pH 8.3, 1 mM EDTA) and adding SYBR green 1 dye (Lonza) to the manufacturers recommended concentration (1x) immediately before measuring the fluorescence. RCA products could be diluted in TAE buffer and then stored in the fridge for several days before diluting a fraction of the products further with TAE and SYBR green 1 dye. Fluorescence was measured in a QM-6 spectrofluorimeter (Photon Technology International) by exciting at 490nm with a 14 watt lamp and recording from 505 nm to 550 nm with a integration time of 0.5 seconds and photomultiplier set to 1000 V. Slit sizes on the monochromators were set to 0.5 mm. Alternatively, the products could be digested by adding 20units of PstI-HF endonuclease (New England Biosciences) and incubating at 37 °C for 1 hr, then separating on an agarose gel. PstI-HF reaction buffer (CutSmart Buffer, New England Biolabs) was added to 1x but was not found to be necessary for successful digestion

*PstI digestion site mutagenesis on Fzz8 phage.* PCR mutagenesis was used to insert an additional PstI recognition site (5'-CTGCAG-3') as a silent mutation into the TetA gene. Briefly, two complementary primers encoding a one bp change in sequence were used to PCR amplify the Fzz8 phage genome using Phusion high fidelity polymerase (New England Biolabs). The PCR products were digested with DpnI endonuclease (New England Biolabs) and was transformed into chemically competent Dh5Alpha cells (New Enlgand Biolabs). Resulting transformants were grown and minipreped and the harvested phage genomes were digested with

PstI to screen for the proper mutation and sequenced. A similar protocol was used for the insertion of a second PstI site on the M13KE based phage used for phage display. Here the second PstI site was inserted as a silent mutation at the N-terminus of the p8 coat protein.

*Anti-Goat Rabbit IgG detection with Fzz8 phage.* 25 ul of 10 mg/ml streptavidin coated magnetic beads (T1, Life Technologies) were diluted in 1 ml of PBS with 0.05% Tween-20 (Sigma). The beads were washed three times by magnetically separating the beads and replacing the buffer three times. Then the beads are resuspended in 250 ul of the same buffer and 25 ul is aliquoted to each 200 ul PCR tube. 1 ul of the biotinylated antigen solution diluted in PBS with 1 mg/ml Bovine serum albumin (BSA), is added to each aliquot. Tubes are vortexed briefly and then left at room temperature for 1 hr with end over end mixing. 75 ul of 1 mg/ml BSA in PBS with 0.05% tween, was added to each tube to block the excess STV sites and the tubes were incubated for another hour. Fzz8 phage was diluted to  $1 \times 10^{12}$  particles/ml in PBS with 0.1% Tween and incubated for 2 hrs at RT with end over end mixing. Beads are magnetically separated from blocking solution and 95 ul of diluted phage solution is added and incubated at room temperature with end over end mixing for 1 hr. Beads are magnetically separated from phage solution and washed with 200 ul of PBS with 0.1% tween 4 times and 100ul of UV irradiated PBS 1 once. 5 ul of UV irradiated water is added to each tube to re-suspend the beads and the RCA reaction is performed using the same protocol as phage alone (detailed above).

*Phage display.* Phage display was performed similar to what has been described previously.<sup>63</sup> A library containing  $1 \times 10^9$  different phage clones expressing random 12mer peptide sequences on their p3 coat proteins was purchased from New England Biolabs and  $1.2 \times 10^{11}$  phage were incubated for 1 hr with 16 pMoles of Biotinylated polyclonal anti-lysozyme antibody produced in rabbit (Rockland Immunochemicals) in TBS. The complexes were then immobilized

on magnetic streptavidin coated beads (Life Technologies) and unbound phage was removed by washing the beads 10 times with TBS containing 0.1%PBST. Bound phage were eluted using Glycine-HCl solution buffered to pH2.2 and amplified in ER2738 cells (New England Biolabs) following the suppliers instructions. The panning procedure was repeated twice more while increasing the tween concentration in the wash buffer to 0.3% and 0.5%. Individual phage clones were isolated and sequenced following the third round of panning and phage expressing unique peptides were tested for affinity to the antigen.

*Peptide cloning to p3 phage coat protein.* Cloning specific peptides to the p3 phage coat protein was accomplished via traditional restriction ligation cloning into the EagI and KpnI that are present at the N-terminus of the mature p3 sequence in M13KE type phage from New England Biolabs. The FLAG and c-Myc peptide epitopes were chosen for their reported ability to bind specific antibodies with high affinity.<sup>115,116</sup> Two complementary oligomers were ordered from Integrated DNA technologies and designed to insert the epitope sequence DYKDDDDK at the N terminus of p3, preceded by the two amino acids DV and connected to the rest of the p3 protein with a tri-glycine linker. The N-terminal DV sequence is the same as in wild-type p3 and was included because previous reports of phage display against the M2 antibody have produced inserts containing the FLAG epitope nested two or three amino acids in from the N-terminus.<sup>117,118</sup> The c-Myc epitope sequence EQKLISEEDLN was similarly cloned with a tri-glycine linker without further modification. Biotinylated anti-c-Myc antibody 9E10 was purchased from Sigma Aldrich. anti-FLAG antibody M2 was also purchased from Sigma Aldrich, but was biotinylated at a 40:1 molar ratio with NHS-biotin (Pierce Biotechnology) and purified with a 2 kDa MWCO mini dialysis cassette (Pierce) before use.

### Section 3.3: Results and Discussion

For our initial experiments, we used an Fd-Tet type bacteriophage (carrying tetracycline resistance) engineered to express a repeated IgG binding Z domain of protein A from *Staphylococcus aureus* fused to its p3 proteins (Fzz8). As a first step, the minimal amount of phage needed to produce detectable amounts of DNA within a few hours was determined. For this, we first heated the phage in the presence of degenerate hexamer primers at 95°C, then added a solution of dNTPs and Phi29 polymerase and incubated the samples at 30 °C before stopping the reaction by heating to 65 °C for 10 minutes.<sup>115,116,119</sup> Though previous work with phage used 10 minute denaturing times to release the phage genome, we found that heating at 95 °C for a minute was not only optimal but that longer heating caused decreases in the subsequent amplification process.<sup>114</sup> In order to remove any background DNA contaminants not part of the phage genome, PCR grade clean tubes and tips were used to handle the amplification solutions. In addition, all buffer solutions were irradiated for 15 minutes under a UV lamp before being added to the primer, polymerase and dNTP solutions. In order to confirm that the amplified DNA correlated to the Fzz8 phage genome, the products were reacted with PstI endonuclease, which cuts at a single site within the viral sequence. Using this protocol, phage concentrations from 339 pM to 33.9 aM could be amplified in three hours and digested to produce a distinct band on an agarose gel as shown in Figure 3.1a. This band migrated at a rate consistent with the predicted ~9500bp dsDNA fragment produced by PstI cutting one site in each phage genome. No other bands were observed in the gel indicating that only the Fzz8 genome was amplified. To better quantify the amplification products, solutions were diluted in TAE buffer containing SYBR green I dye and their fluorescence was measured. The fluorescence peak intensity increased with

higher amounts of initial phage used and also correlated with the band intensities seen by agarose gel electrophoresis (Figure 3.1b).

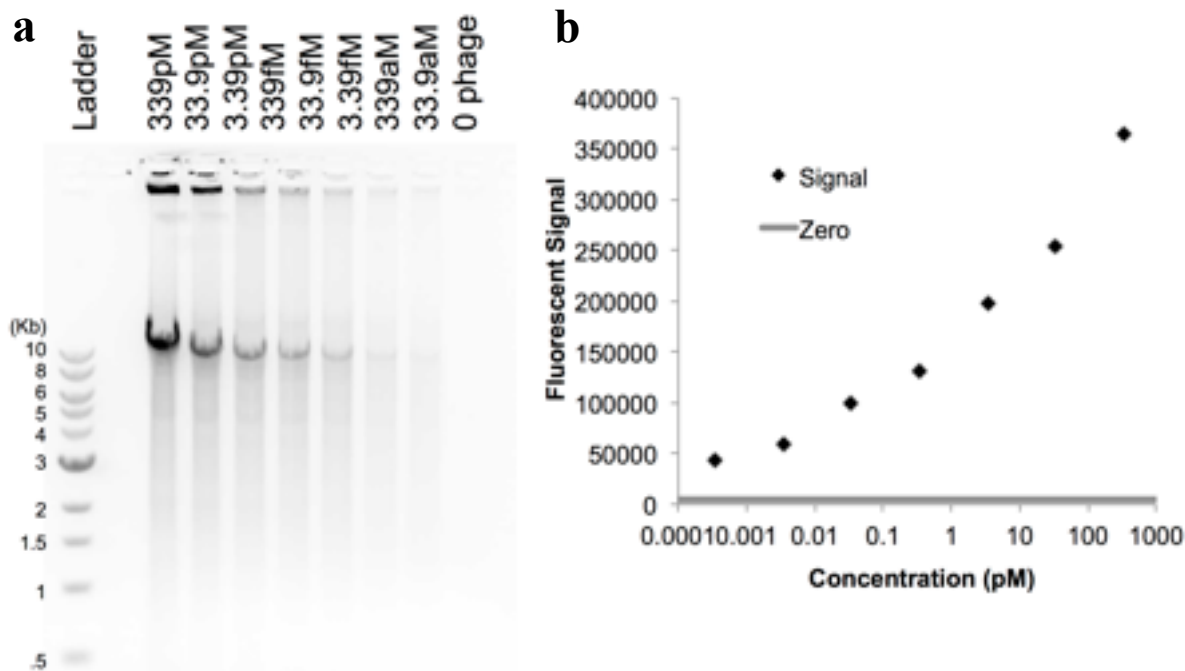


Figure 3.1. a) Rolling circle amplification products from the indicated phage concentration then digested with PstI endonuclease and run on an ethidium bromide stained agarose gel along with a DNA ladder. Largest DNA ladder band is 10 kilobases. b) Products quantified by fluorescence after mixing with SYBR green I dye.

In order to see if the viral genome could be used to type different antigens in solution, we decided to run RCA reactions from phage that contained genomes that differed from each other in terms of the number and locations of the PstI cut sites. For this, we first inserted a second PstI site in the Fzz8 DNA to generate two types of phage which either contained one or two PstI cut sites. We then ran RCA reactions from mixtures of these two types, followed by a PstI digest and agarose gel electrophoresis. As shown in Figure 3.2, the relative phage concentration of each type corresponded to the intensity of the bands digested from the amplification products. This was also corroborated by ImageJ analysis of the fluorescent intensities of the bands (Figure 3.3).

Though sequence bias has been shown to occur with RCA due to differences in secondary structure of the template and products,<sup>120,121</sup> the two 9500bp long phage genomes only differ in a single base, so sequence based amplification biasing is highly unlikely to occur. It should however be noted that there was a significant amount of fluorescence visible in the wells loaded with each digest. This was seen in all amplifications and we hypothesize that this is caused by either parts of the hyperbranched products not becoming linearized with PstI, or by the highly processive Phi29 polymerase still binding to some part of the products. It is unlikely that this is simply caused by undigested concatemers since extending the digest time or increasing the endonuclease concentration did not decrease the intensity of fluorescence in the well.

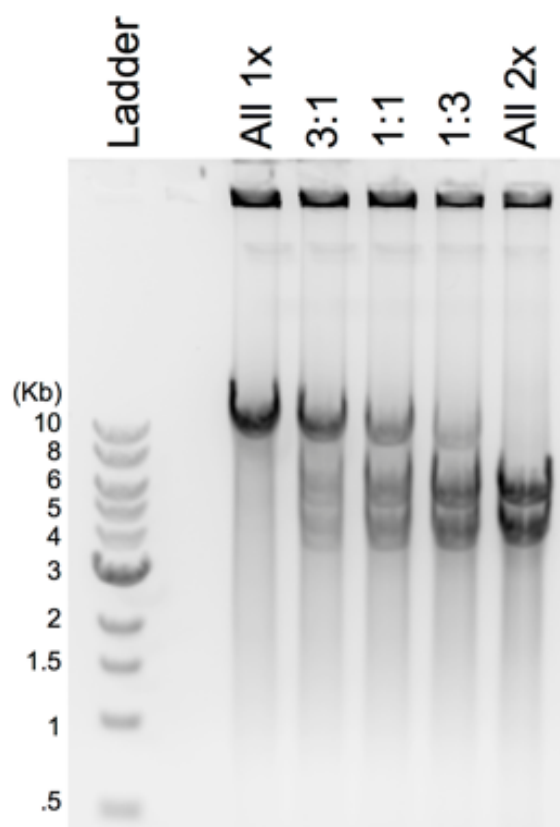


Figure 3.2. Whole phage particles bearing 1 or 2 PstI recognition sites (1x or 2x) within their genome were mixed at the indicated ratio such that the total phage particle concentration was 339 pM and then amplified with RCA. Amplification products were digested with PstI endonuclease and ran on an ethidium bromide stained agarose gel.

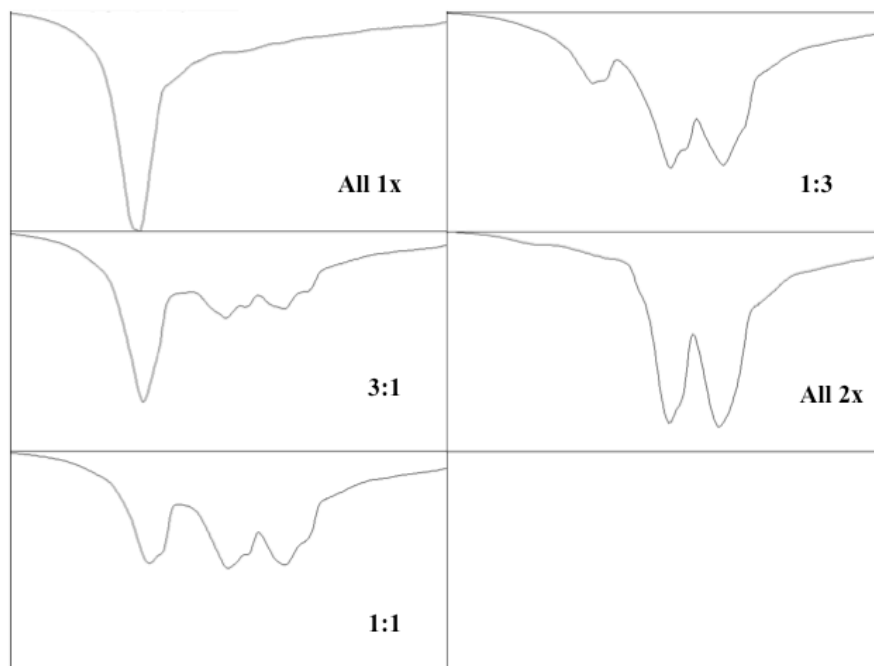


Figure 3.3. Gel analysis of Figure 3 with ImageJ software showing fluorescence intensity moving down each gel lane.

To demonstrate the utility of phage as biosensor probes, we first tested the use of Fzz8 for detecting rabbit IgG1 through binding of the repeated Z domain to the Fc portion of the antibody. The Z domain is known to bind rabbit IgG1 with a dissociation constant slightly higher than the nM range with which it binds human IgG1.<sup>122,123</sup> In the assay, varying concentrations of biotinylated rabbit IgG1 were first bound to streptavidin functionalized magnetic beads in PCR tubes and then probed with a solution of 1.67 nM Fzz8 phage whose genome contained a single PstI cut site. Non-specifically bound phage were removed by washing several times with a 0.1% tween solution. The RCA reactions were next run directly from the phage coated beads by first adding the primers directly to the same PCR tubes and heating at 95 °C followed by the polymerase, dNTPs and heating at 30 °C for 2 hours. The RCA products were then mixed as before with SYBR green and the fluorescence output of each tube was measured. As shown in

Figure 3.4, the RCA reactions allowed us to detect down to  $\sim 3$  pM of rabbit IgG in solution demonstrating the high sensitivity of the assay. The RCA products were also digested with PstI and characterized by gel electrophoresis to demonstrate that the phage genome was the amplified product.

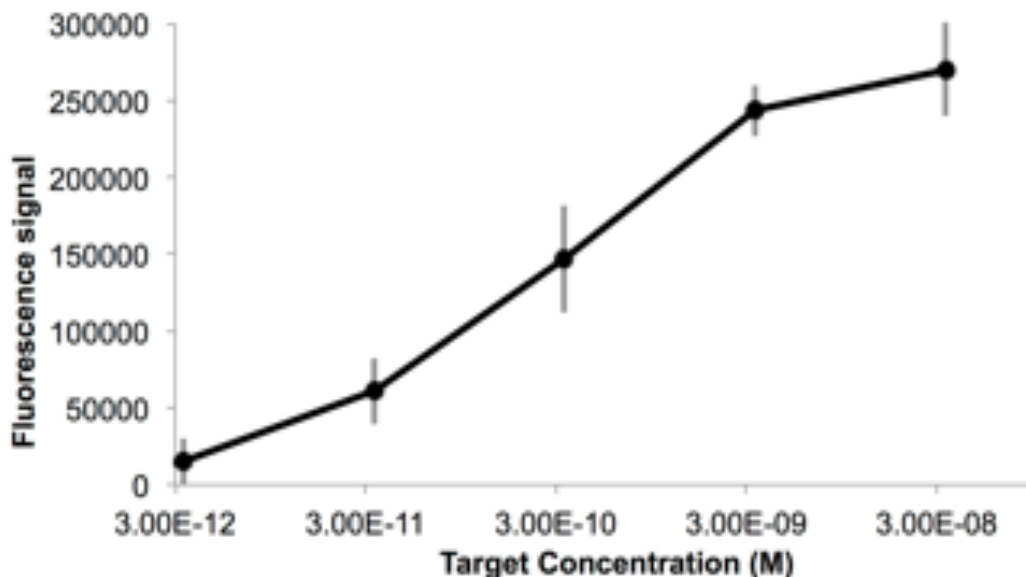


Figure 3.4 Results of an assay for Rabbit IgG using phage expressing the antibody binding ZZ domain as RCA probes. Signals represent averages and standard deviations of four assays normalized to the no-target control in each assay. Amplification products are quantified by mixing with SYBR green 1 dye.

In order to compare the RCA results with phage ELISA data, we first reacted Fzz8 phage with beads coated with different concentrations of rabbit IgG. Next, we added horseradish peroxidase (HRP)-conjugated anti-Fzz8 (anti-M13) antibodies (GE Healthcare) and developed a signal with 2,2'-azino-bis(3-ethylbenzothiazoline-6-sulphonic acid) (ABTS). As shown in Figure 3.5, the phage ELISAs gave comparable detection limits to those observed with the RCA reactions. Phage ELISA is known to be very sensitive because each virus can bind multiple anti-Fzz8 (anti-M13) antibodies, each of which in turn has multiple HRP enzymes. However, in

contrast to phage ELISA, using RCA does not require the use of additional detection antibodies. Furthermore, because each phage genome can be typed to a specific analyte, different antigens can be identified in a single solution, which is also not possible with ELISA.

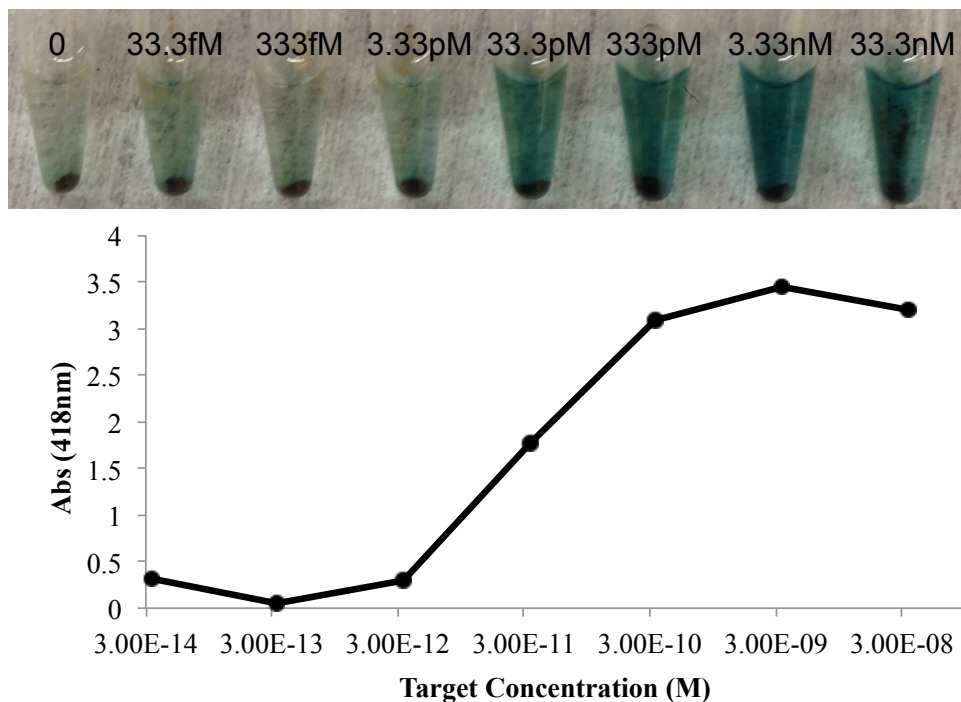


Figure 3.5. Results of an ELISA for Rabbit IgG using phage expressing the antibody binding ZZ domain as RCA probes. Since the absorbance values become very small below 3.33 pM target, similar signals are obtained at these low antigen concentrations.

Next, in order to use phage RCA to detect and identify multiple proteins simultaneously, we created three types of phage, each capable of binding different proteins with high specificity. Each set of phage was designed to contain different patterns of PstI recognition sites within the genome. For multiplexed sensing, we first produced phage that recognized anti-FLAG, anti-cMyc and anti-lysozyme antibodies. For the anti-FLAG and anti-cMyc targets, we cloned specific peptides that are known to bind the two different antibodies as fusions to the p3 proteins.<sup>124,125</sup> The phage that recognized anti-lysozyme antibodies were isolated by phage

display. Sequencing of ten plaques eluted from a fourth round of panning against anti-lysozyme gave the consensus sequence TDFNTMAKNNPP. All three types of phage were next tested in ELISAs for binding to anti-lysozyme, anti-FLAG, and anti-cMyc and in all cases, each phage type was found to bind only to their specific targets with minimal cross-reactivity. To gauge the binding affinity of each phage against their specific targets, ELISAs were performed with serial dilutions of each target. Based on these results (Figure 3.6), the anti-FLAG binding phage showed the highest affinity while anti-lysozyme binding phage showed the lowest.

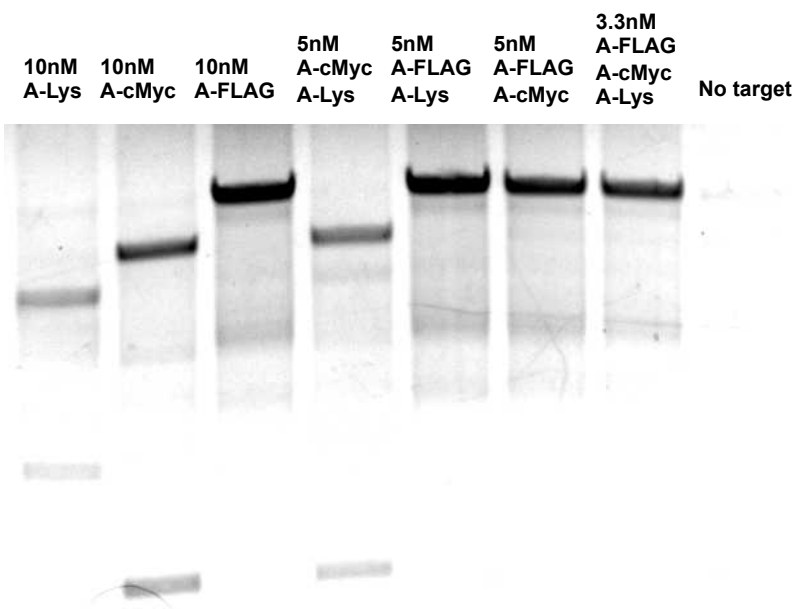
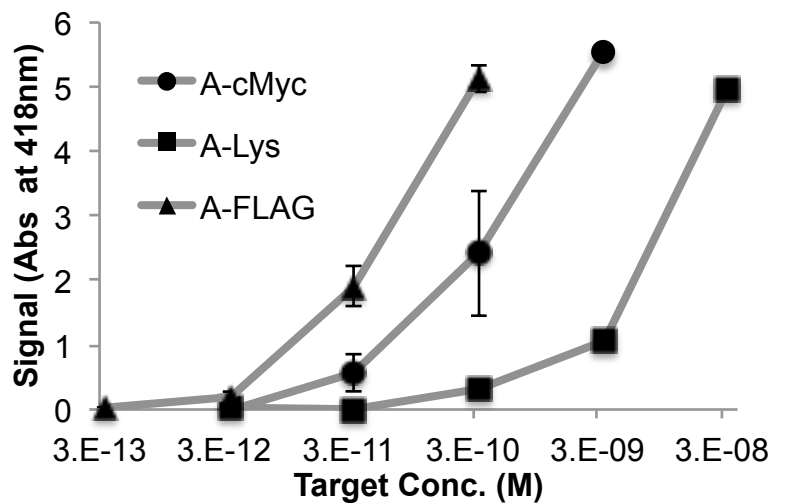


Figure 3.6. (Top) Comparison of three ELISAs using peptide bearing phage at a concentration of 1.66 nM to probe varying concentrations of their respective targets. Results are listed by target. Bound phage were detected with an anti-M13 HRP conjugate. (Bottom) Gel electrophoresis results using equal molar concentrations (~550 pM) of each phage type.

In order to differentiate the phage genomes, PCR mutagenesis was used to modify the DNA of the anti-lys and anti-cMyc binding phage by making silent mutations at different points. A second PstI site was made in the p8 and p4 coding sequences for anti-lys and anti-cMyc

binding phage, respectively. This was designed so that after the PstI digest, the anti-lys binding phage would produce two fragments composed of 4876 and 2345 bases while the anti-cMyc binding phage would produce two fragments composed of 5847 and 1375 bases. The anti-FLAG binding phage was designed to contain a single PstI site. Successful mutations were confirmed by digest and gel electrophoresis, and all mutated genomes produced phage with no noticeable loss in efficiency. Next, ~550 pM solutions of the three different sets of phage were used to detect varying amounts of the three biotinylated targets mixed in a single solution. For this, we first reacted the streptavidin-coated beads with 10 nM solutions that contain a single antigen or a mixture of the three different proteins. After the unbound phage were removed by washing, RCA reactions were run for 2 h and the products were measured by photoluminescence and agarose gel electrophoresis. When starting from equimolar amounts of the three different sets of phage in solution, the RCA products gave the same fluorescence output. However, the gel electrophoresis results revealed that the varying phage affinities for their specific antibody targets greatly affected the detection limits for each antigen in that the phage that had the highest affinity for the antigen tended to dominate the gel results. For example, since the anti-FLAG binding phage demonstrated much higher binding affinity than the anti-lys binding phage, the RCA product from the anti-FLAG binding phage was overwhelmingly brighter than that obtained from the anti-lys binding phage gel electrophoresis despite the equal loadings of antigens in solution. Thus, the brightness of each band did not correlate with the actual antigen concentrations (Figure 3.6).

Because of difficulties in creating phage with equal affinities for each target, we decided to tune the starting concentrations of each phage type in the assay to match their specific binding affinities. Since the anti-FLAG binding phage clearly showed the highest affinity by ELISA

(Figure 3.6), we lowered the starting anti-FLAG phage concentration to 1.66 pM. The anti-cMyc binding phage showed ~100 fold lower affinity than the anti-FLAG phage and ~10 fold higher affinity than the anti-lysozyme binding phage so their concentrations were changed to 166 pM and 1.66 nM, respectively. The average concentration of the entire phage mixture was thus ~610 pM, similar to the concentration used in the previously described assay (Figure 3.6). Next, the phage were mixed at varying dilutions with the beads coated with different antigens, followed by RCA, photoluminescence measurements (Figure 3.7) and gel electrophoresis (Figure 3.8). By matching the starting phage concentration to their relative binding affinities for the targets, we were able to see that DNA band intensities obtained now correlated to the starting concentrations of antigens in solution (Figure 5). This relationship was also confirmed by ImageJ analysis. It is also important to note that the assays were highly specific to the particular antigens tested, meaning no extraneous bands were observed in the absence of a specific target.

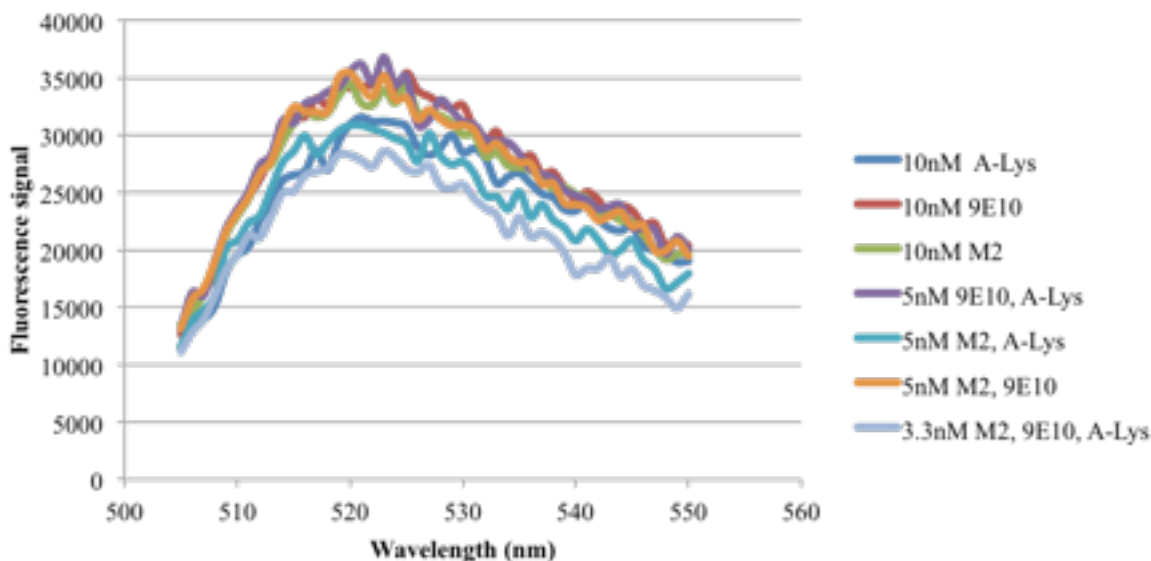


Figure 3.7. Fluorescence signals above background for RCA products created in the assay shown in Figure 5.

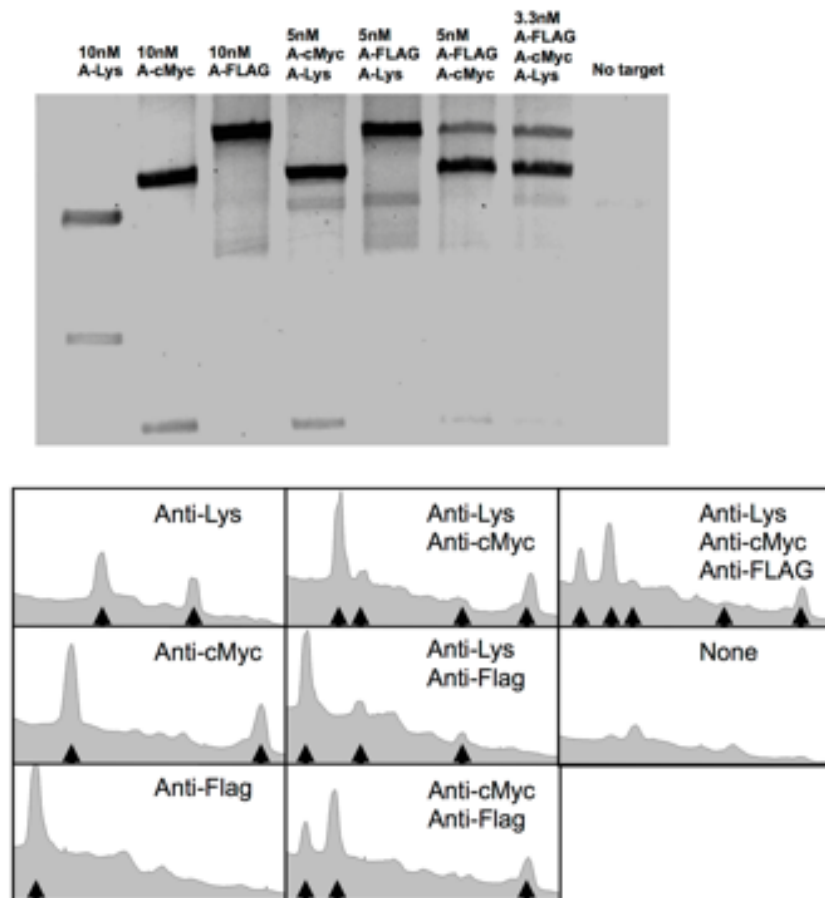


Figure 3.8. (Top) Gel electrophoresis results of using an unequal mixture of the three phage sets to detect mixtures of targets at the indicated concentrations. The phage concentrations used were based on the relative affinities determined by phage ELISAs. The concentrations of the anti-lysozyme, anti-cMyc and anti-FLAG binding phage were at 1.66 nM, 166 pM and 1.66 pM respectively. (Bottom) imageJ analysis of gel shown. Peaks corresponding to bands created from phage products are indicated with arrows.

### Section 3.4: Conclusions

In conclusion, we have demonstrated the use of engineered bacteriophage as probes to detect multiple antigens in solution using the contained viral genome as a detectable agent. The large genome of the virus was easily amplified via RCA, and could be engineered to not only express specific binding domains (peptides, antibodies) to particular antigens, but also contain restriction enzyme sites for antigen typing by gel electrophoresis. This method allowed sensing for different antigens in solution without expensive fluorescent-nucleic acid probes or a patterned

surface. We show that the isothermal phage RCA reactions yield sensitivities similar to those obtained via phage ELISAs, but without antibody or enzyme conjugates. Finally, we demonstrate that despite different affinities for protein targets, the initial phage concentrations could be altered to obtain quantification of multiple analytes in solution. In future work, we will study ways to minimize the differences in phage binding affinity by using phage-antibodies using non-canonical amino acids for covalent photo-conjugation of antibodies to the ZZ domain expressed on Fzz8.<sup>126,127</sup>

## Chapter 4

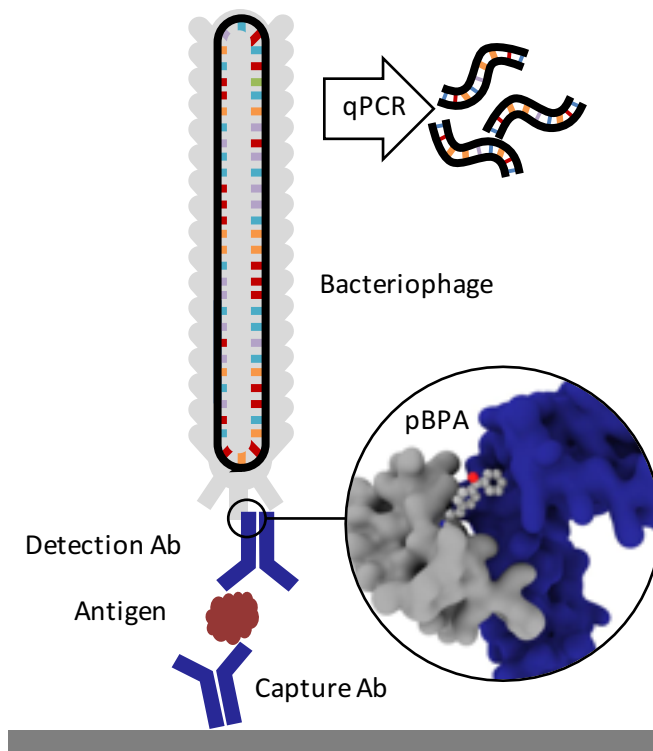
### Antibody phage conjugates as qPCR probes

#### Section 4.1: Introduction

The detection of specific biomarkers with high sensitivity is critical for early diagnosis and treatment. Because many key protein biomarkers are found at concentrations below the detection limits of standard enzyme linked immunoassays (ELISAs), new diagnostic tools are continuously being sought.<sup>128-130</sup> One strategy has been to use immuno-PCR, which first requires labeling detection antibodies with oligonucleotides and utilizing polymerase chain reaction (PCR) to generate amplified signals in response to a single antigen binding event.<sup>102,104,105</sup> Because each antibody can be labeled with a distinct nucleic acid sequence, immuno-PCR can potentially be used for multiplexed analysis.<sup>130</sup> However, a significant drawback of immuno-PCR is that covalent conjugation of DNA to antibodies can not only hamper the affinity and specificity of the antibody to its antigen but also lead to highly heterogeneous populations of antibody-DNA conjugates.<sup>131</sup> This can lead to varying, erroneous, or large background signals.<sup>103</sup> While antibodies expressed recombinantly can potentially be site-specifically modified, many sequences of clinically relevant antibodies are often unknown, and recombinant expression frequently leads to lower antigen affinities.<sup>103,114,132</sup> As such, these methods are often difficult to apply for immuno-PCR.

As a means of overcoming these issues, we demonstrate here the use of genetically engineered bacteriophage encasing a multi-kilobase circular genome that can be amplified to detect and identify specific antigens in solution. Because the amplifiable phage DNA is well-protected within the phage capsid, it neither interferes with nor impedes the antigen binding

event (Scheme 4.1). Furthermore, the phage capsid can protect the DNA from being degraded by enzymes such as DNase that may be present in a conventional clinical sample.<sup>133</sup> To fabricate the antibody-phage constructs, we show here methods to covalently attach the constant fragment (Fc) region of monoclonal detection antibodies to phage by expressing an antibody binding peptide on the p3 capsid proteins that also incorporate the photocrosslinkable non-canonical amino acid p-benzoyl-L-phenylalanine (pBPA) (Scheme 4.1). By introducing covalent crosslinks between the antibody and the phage, nonspecific binding of the phage to other antibodies in solution or on a surface was effectively eliminated. To use the phage genome to type and quantify the antigen in solution, the DNA of each antibody-phage construct was modified to recognize specific primer sets used to amplify portions of the viral DNA. Since each primer set will only amplify one specific phage sequence, multiplexed detection of several biomarkers in solution could be performed in real time by employing a universal Taqman probe (Scheme 4.1). Immunoassays run from the antibody-phage conjugates showed low pg/ml detection limits of three different cancer biomarkers in a single solution in fetal bovine serum.



Scheme 4.1: Depiction of immuno-PCR enabled by photo-crosslinked antibody-phage conjugates. Phage express a antibody binding peptide containing a photocrosslinking non-canonical amino acid (pBPA) which crosslinks with detection antibodies used in a sandwich immunoassay. The phage genome then acts as a template for quantitative PCR.

## Section 4.2: Methods

*Phage design and production.* The genome of phage fUSE5 was modified using standard molecular cloning techniques to insert two concatenated copies of the antibody binding peptide (Z domain) or a single copy with the stop codon (TAG) substituted for Q32 as fusions to the N-terminus of capsid protein p3<sup>85</sup>. A PCR mutagenesis reaction was then used on the genome bearing two copies of Z domain to generate versions bearing the Q32 mutation within one or both copies. Phage bearing these mutations were produced by transforming *E.coli* with both the modified phage genomes as well as the pEVOL-pBpF plasmid. The pEVOL-BpF plasmid was procured from Addgene which contained both the orthogonal tRNA and amino acyl RNA synthetase required for translation of p-benzoyl-L-phenylalanine (pBPA) at amber stop

codons.<sup>134,135</sup> Transformants were selected on Tetracycline and Chloramphenicol containing plates before being pricked and amplified in 40 ml of LB containing ~300  $\mu$ M pBPA, 20  $\mu$ g/ml Tetracycline, 50  $\mu$ g/ml Chloramphenicol and 0.1% Arabinose for the induction of the pEVOL-pBpF. Phage were amplified from the transformants for approximately 20 hr, after which cultures were spun at 10,000g to remove *E.coli* from the phage laden supernatant. Phage were precipitated from the supernatant through the addition of a solution of 20% weight per volume 8,000 MW PEG in 2.5M NaCl at a 1/5<sup>th</sup> volumetric ratio followed by incubation at 4 °C overnight and centrifugation at 10,000g for 15 min. The resulting phage pellet was re-suspended in 1 ml of PBS (pH 7.6) and spun at 22,000g for 5 min to remove remaining cellular debris. Phage were precipitated again for 1 h followed by centrifugation at 22,000 g for 15 min. The phage pellet was then re-suspended in 200  $\mu$ l of PBS and stored at 4 °C until use. Phage concentration was determined by UV spectrophotometry.

*Photo-conjugation and Characterization of Antibody-Phage via ELISA and SDS PAGE gel.* Phage were diluted to a final concentration of  $2.5 \times 10^{13}$  phage/ml in PBS and mixed with a 1:10 molar excess of mouse IgG1 clone Mab1 raised against recombinant TNF $\alpha$  (eBioscience). Antibody-phage mixtures were then transferred to a 0.6 ml polypropylene tube and placed ~1.5 m in under a 365 nm UV lamp such that the power received was measured to be 810  $\mu$ W/cm<sup>2</sup>. Phage antibody conjugates were irradiated for 3 h. The extent of conjugation was determined by denaturing irradiated antibody-phage mixtures and separating them on an SDS PAGE gel (Novex 4-12% BisTris gel, Life Technologies). ELISA was used to measure antibody-phage conjugate affinity by first suspending 25  $\mu$ g of streptavidin functionalized magnetic beads (Dynabeads myONE streptavidin T1, Life Technologies) in a 25  $\mu$ l solution of 133 nM biotinylated antiTNF $\alpha$  (Mab11, eBioscience) or 32 nM biotinylated recombinant TNF $\alpha$  (eBioscience) in 0.05% PBST.

These coated beads were then mixed with the antibody-phage conjugate solutions diluted in 0.1% PBST such that the final phage concentration was 1.6 nM. Beads were washed twice with 0.1% PBST and bound antibody-phage conjugates were detected by the addition of an antiphage antibody conjugated to HRP (horse radish peroxidase) (GE healthcare) followed by two more washes and the HRP substrate ABTS (2,2'-Azinobis [3-ethylbenzothiazoline-6-sulfonic acid]).

*Immunoassays using photo-conjugated antibody-phage construct.* Immunoassays were done with antibody-phage conjugates that were irradiated as above for 14 h in the presence of antibody at 20:1 antibody:phage molar ratios. Unbound antibody was then removed by PEG precipitating the phage from solution and re-suspending to  $1 \times 10^{12}$  phage/ml in 0.1% PBST. In the immunoassays for only a single antigen, 25  $\mu\text{g}$  of streptavidin functionalized magnetic beads were suspended in a 25  $\mu\text{l}$  solution of 133 nM biotinylated capture antibody (purchased from Invitrogen for anti-IL6 or IL1 $\beta$ , eBioscience for anti-TNF $\alpha$ ) for 1 h followed by blocking with fetal bovine serum (FBS) (Sigma Aldrich) for an additional hour. Targets were then diluted to the indicated concentration in FBS and incubated with the coated and blocked beads for 1 h. Beads were removed from the target solution and re-suspended in the antibody-phage conjugate solution for 1 h followed by four washes with 0.1%PBST to remove un-bound conjugates. One fifth of the beads were then used for PCR analysis by diluting them in Taqman universal mastermix II (Life Technologies) along with phage specific primers (600 nM) and Taqman probe (250 nM) (Integrated DNA Technologies). Quantitative PCR was then performed in an Applied Biosystems QuantStudio6 Flex real time PCR system. Threshold change in normalized fluorescence was set to 0.5 for all results shown. The multiplex protocol was performed identically except that each assay was done with a mixture of beads bound to three different capture antibodies under the same ratios as above (still using 25  $\mu\text{g}$  of beads total per assay), and

a mixture of antibody-phage conjugates (each at  $1 \times 10^{12}$ /ml) was used to detect the targets rather than just one.

### Section 4.3: Results and Discussion

In order to fabricate the antibody-phage constructs, filamentous phage were utilized due to their tolerance for genetic modification, ability to grow to high titers in *E. coli* and the relatively small size as compared to other strains.<sup>15,113</sup> The viruses grow from a single stranded circular DNA genome that becomes packaged into the viral capsid which contains distinct capping proteins at either end. One end of the phage expresses 3 to 5 copies of the p3 protein which are often used to express peptides, or single chain variable fragments that bind particular targets.<sup>19,64,65</sup> In order to attach antibodies to the phage, we have recently developed methods to express a protein A domain (Z domain) from the p3 proteins which can non-covalently associate with the Fc portions of detection antibodies.<sup>136</sup> While this does allow producing antibody-conjugated phage, the non-covalent and relatively low affinity interactions between the Z domain and the antibody can lead to antibody dissociation from the phage leaving an unoccupied Z domain.<sup>44,87</sup> This event would then allow the virus to bind another antibody in solution or on a surface, making multiplexed detection difficult or lead to high background signals. Therefore, in order to introduce covalent bridges between the Z domain on the phage and the Fc portion of the detection antibodies, a non-canonical amino acid p-benzoyl-L-phenylalanine (pBPA) was inserted at position glutamine 32 (Q32) on the Z domain through Amber codon suppression. This amino acid site was chosen based on previous studies by Hui *et al* who showed that this led to optimal crosslinking between the Z domain and mouse IgG1 antibodies.<sup>126</sup> In order to test if having multiple Z domains expressed per p3 protein led to higher affinities to antibodies, phage were

designed to express either a single copy of a pBPA incorporated Z domain, two consecutive copies, or two consecutive copies with only one of the two Z domains containing a pBPA substitution. Also, a phage expressing two copies of the Z domain without pBPA was used as a control. Phage genomes were modified to produce these constructs by restriction ligation cloning and PCR mutagenesis, and confirmed via sequencing (Supporting Information).

After producing the phage in *E. coli* and purifying via PEG precipitation, all of the different types of pBPA-Z domain expressing phage were irradiated under a 365 nm UV lamp in the presence of the antibody anti-tumor necrosis factor alpha (anti-TNF $\alpha$ ) at a 10:1 molar ratio of antibody:phage. As a control, phage were photoirradiated in the absence of antibody. The resulting conjugates were first characterized through denaturing SDS PAGE which showed higher molecular weight bands corresponding to an antibody crosslinked to either one or two p3 fusion proteins (Figure 4.1). These bands were only present when antibody was added to the phage and irradiated. Furthermore, the addition of antibody to control phage that expressed Z domains with no pBPA amino acid did not yield any corresponding high molecular weight bands in the gel (Figure 4.1). Previous crystallographic studies have shown that each antibody has two possible Z domain binding sites within the Fc region which may explain the presence of the band that corresponds to the an antibody bound to two p3 fusion proteins.<sup>137</sup> The strong intensity of this band may be due to the p3 proteins being in close proximity to one another on the phage tip, making it more likely that a previously crosslinked antibody will be crosslinked again.

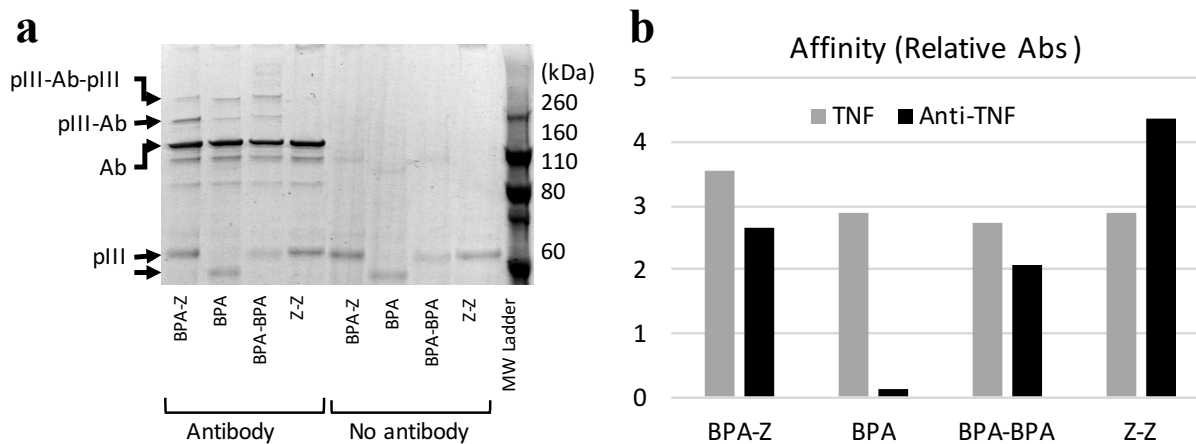


Figure 4.1: Phage were made to display on their p3 proteins two repeated Z domains containing the photo-crosslinking non-canonical amino acid pBPA on both (BPA-BPA) one (BPA-Z) or neither copy (Z-Z). A fourth phage was made to express only a single copy containing pBPA (BPA). a) Phage were irradiated with or without Anti-TNF $\alpha$ , denatured and separated on a polyacrylamide gel shown. b) The same antibody-phage conjugates were tested for binding affinity to TNF $\alpha$  or additional anti-TNF $\alpha$  via ELISA using an anti-phage antibody conjugated with HRP.

In order to utilize the antibody-phage conjugates in immunoassays, it is critical that the constructs not only possess high affinity for the antigen but also that non-specific binding to other antibodies in solution or on a surface be completely eradicated. In order to test the photo-crosslinked anti-TNF $\alpha$ -phage for binding to either TNF $\alpha$  or any capture anti-TNF $\alpha$  antibodies on a surface, phage ELISAs were run. For this, the antibody-phage conjugates were reacted against magnetic beads bound with either anti-TNF $\alpha$  antibodies or TNF $\alpha$  followed by washing to remove unbound conjugates. Next horseradish peroxidase (HRP) conjugated anti-M13 antibodies were added to detect any anti-TNF $\alpha$ -phage bound to the surface. As shown in Figure 4.1b, both the photo-crosslinked and non-crosslinked antibody-phage conjugates show comparable affinities to TNF $\alpha$ , as expected. However, out of the different antibody-phage constructs made, only the phage that expressed a single pBPA substituted Z domain showed almost no affinity to the capture antibodies on the surface. While these results were somewhat

unexpected since the gel electrophoresis analysis (Figure 4.1a) showed that all of the antibody-phage constructs tested have some p3 proteins that are not covalently attached to an antibody, it is clear from the ELISA studies that having a single Z domain per p3 protein is ideal for limiting non-specific binding.

The antibody-phage constructs were also irradiated for longer periods of time to see if this caused further reduction in non-specific binding. As shown in Figure 4.2a and 3.2b, gel electrophoresis shows that after 3 h, the phage is well crosslinked to the detection antibody and minimal non-specific binding to capture antibody on a surface is observed. However, increasing the photoirradiation times to 14 h showed a further decrease in binding to the surface bound antibodies. Interestingly, phage irradiated for 14 h in the absence of any detection antibody also showed minimal binding to additional antibodies, indicating that some other mechanism other than steric hindrance is preventing additional antibody binding. However, these diminished binding affinities of the 14 h irradiated antibody-phage to anti-TNF $\alpha$  did not lead to any decreases in affinity for the antigen TNF $\alpha$  (Figure 4.3).

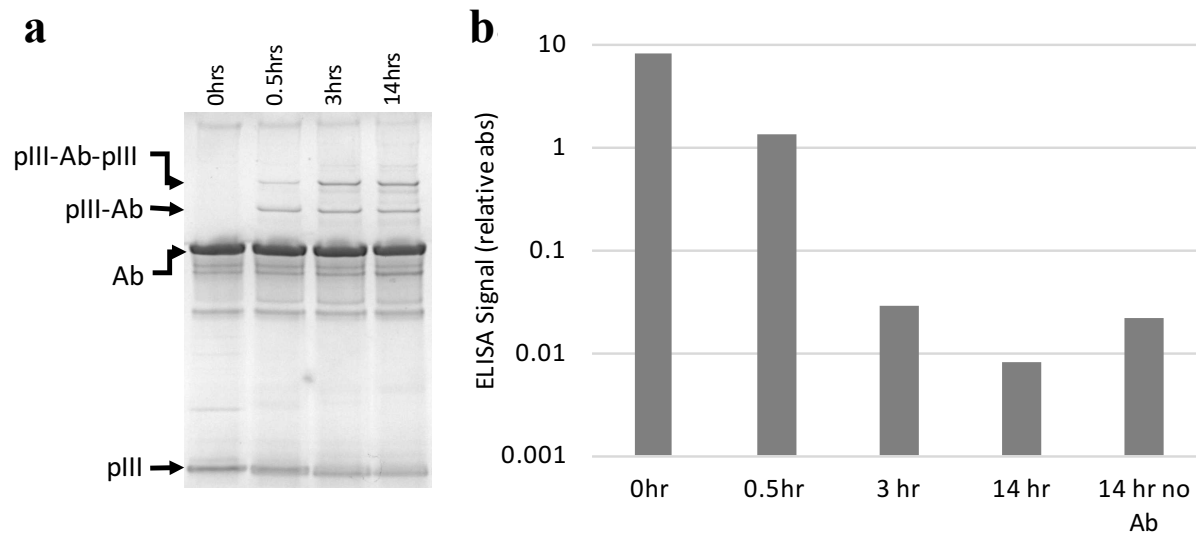


Figure 4.2: Phage expressing only a single Z domain containing pBPA were mixed with anti-TNF $\alpha$  and irradiated for the number of hours listed. The resulting conjugates were denatured and separated on a poly acrylamide gel (a) or tested for binding affinity to additional anti-TNF $\alpha$  (b).

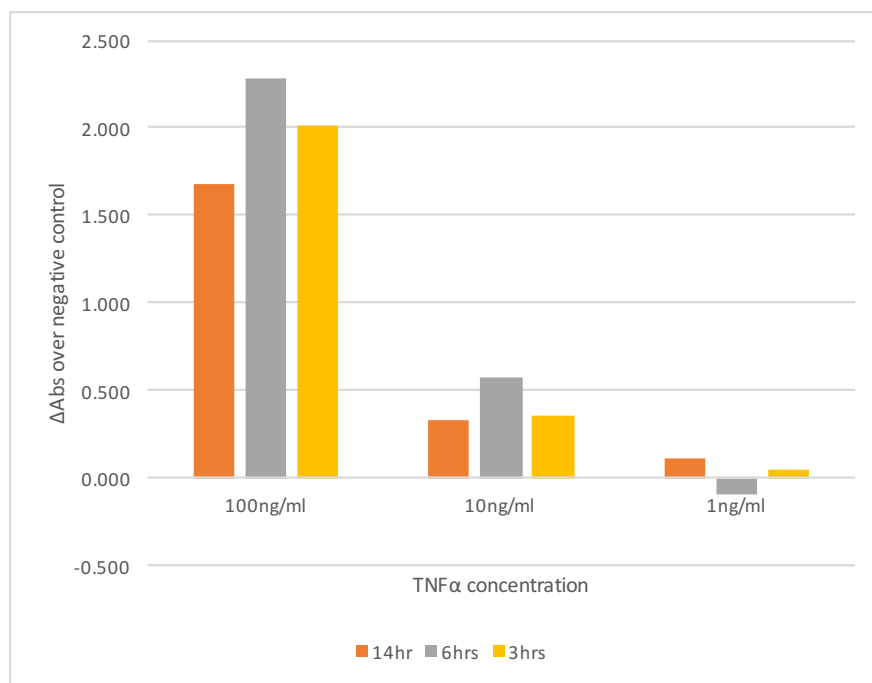


Figure 4.3: Anti-TNF $\alpha$ -phage binding to TNF $\alpha$  after 3 hr, 6 hr and 14 hr photoirradiation. Phage irradiated for indicated amounts of time with anti-TNF $\alpha$  then used to detect various concentrations of TNF $\alpha$  immobilized on magnetic beads. Results show difference in ELISA signal over no TNF $\alpha$  control.

Next, the antibody-phage constructs were tested as scaffolds for immuno-PCR assays. For this, different concentrations of TNF $\alpha$  ranging from 100 ng/ml to 0.1 pg/ml were reacted in fetal bovine serum (FBS) with streptavidin coated magnetic beads that had been pre-reacted with biotinylated anti-TNF $\alpha$  capture antibodies. After removing free antigen, 1e11/ml solutions of the anti-TNF $\alpha$ -phage were reacted with the beads in PBST for 1 h followed by washing away unbound antibody-phage and rinsing 4 times in PBST. Next, PCR reactions were run by resuspending the beads in a PCR reaction mix that contained primers (Table 4.1), polymerase, dNTPs and reaction buffer and submitted to 25 cycles of amplification. The resulting PCR products were then detected by agarose gel electrophoresis (Figure 4.4). Although an amplification product was observed for zero antigen which was likely due to nonspecific binding of phage conjugates to the beads themselves, there was a clear trend in amplification intensity with TNF $\alpha$  concentration and sensitivities down to  $\sim$ 0.1 pg/ml TNF $\alpha$  could be obtained.

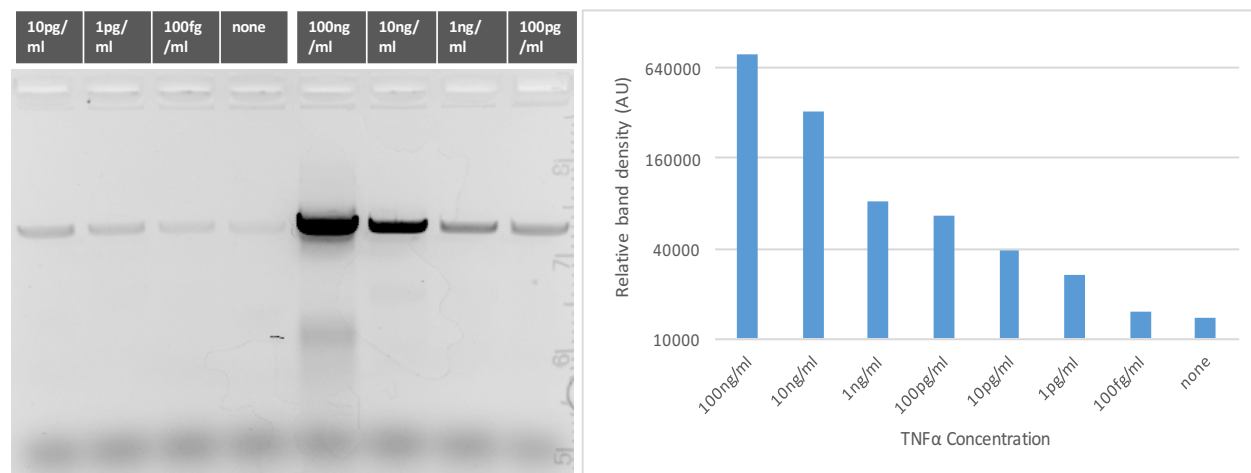


Figure 4.4: Gel electrophoresis based assay for detecting TNF $\alpha$ : Anti-TNF $\alpha$ -phage were used to detect various concentrations of TNF $\alpha$  diluted in 0.1%PBST solution with 5 mg/ml BSA. Immunoassays were otherwise performed as reported in materials and methods. PCR was performed in a standard thermocycler for 25 cycles by adding assay beads directly to PCR reaction mixture containing primers, dNTPs and polymerase. After PCR reaction, reaction mixtures were added directly to a 0.75% agarose gels and electrophoresed for 30min at 120V. Samples are placed in the gel out of order to avoid any gel effects.

Name/description	Sequence
fwd primer 1	Tacctgaacacaagtgcg
fwd primer 2	TcttgaacaggttctagcggAA
fwd primer 3	CTTtcatgtgaactgaggtacgAA
rev primer for all phage	AAgccgcggtaaatagcaataa
universal taqman probe	FAM-ATGCGAAAAACCTAAAAGAGCTTGCCGA-ZEN

Table 4.1: Sequence of primers used for Taqman probe based qPCR. Lower case bases are unique sequences inserted into phage.

Although sensitive, gel electrophoresis is slow to run, laborious, less quantitative and cannot be performed in real-time, so we next chose to test the antibody-phage conjugates in real-time PCR assays. For this, although a DNA staining dye such as SYBR Green could be used, because these dyes can also cause high background signals due to binding to primer dimers for example, a universal Taqman probe was utilized instead. Since Taqman probes are designed to produce signal only upon binding to the PCR template during polymerization, high sensitivities can be obtained and in real-time. For this, we designed a 29mer probe that was complementary to a sequence of the amplified product (but separate from the sequence domains that recognized the primer sets) and also contained a 5' FAM dye, a 3' IBFQ quencher and an internal quencher 9 bases in from the 5' end (Table 4.1). First, this Taqman probe was used to measure amplification in real time starting from various concentrations of phage in solution and also in the presence of magnetic beads which would later be used as an immunoassay substrate. As shown in Figure 4.5a and 4.5b, real-time PCR analysis showed that we could successfully detect down to attomolar concentrations of phage. Next, we ran a real-time PCR immunoassay against varying concentrations of TNF $\alpha$  using the photocrosslinked anti-TNF $\alpha$ -phage following the same procedures described earlier for the gel electrophoresis analysis. As shown in Figure 4.6, real-

time analysis showed that we could detect down to  $\sim 10$  g/ml TNF $\alpha$  in solution. The delta threshold cycle ( $\Delta C_t$ ) values are the difference in threshold cycle for that concentration of antigen versus zero antigen. Therefore, the more sensitive the assay or the lower  $K_D$  between antibody and antigen, larger  $\Delta C_t$  values would be obtained for a given amount of antigen.

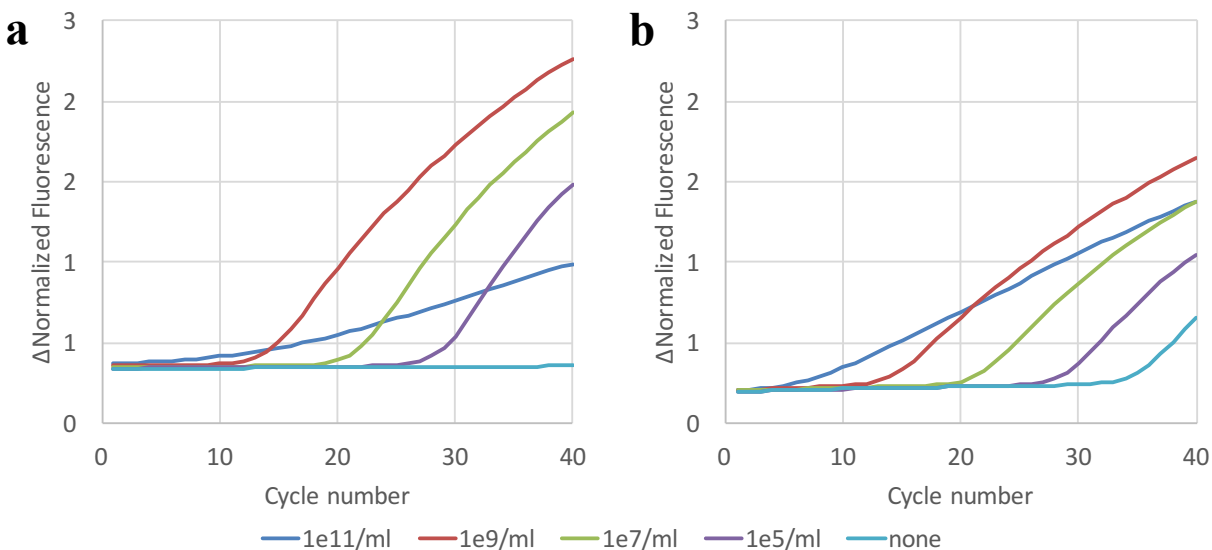


Figure 4.5: Validation of Taqman probes for real time PCR detection of phage in the presence of immunoassay magnetic beads: a) Indicated concentrations of phage are added to a real time PCR reaction mixture containing Taqman universal mastermix II (Life Technologies) along with phage specific primers (600 nM) and Taqman probe (250 nM) (Integrated DNA Technologies). b) Reactions were supplemented with 5  $\mu$ g of streptavidin functionalized magnetic beads (Dynabeads myONE streptavidin T1, Life Technologies).

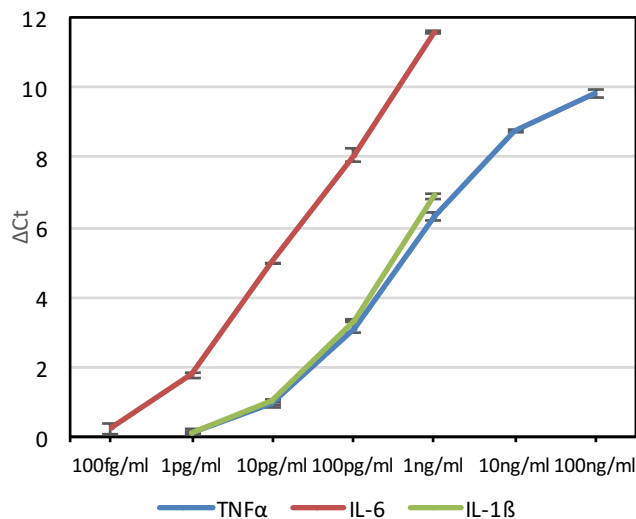


Figure 4.6: Phage are conjugated with antibodies for the three targets listed and used to detect dilutions of said target in a sandwich type immunoassay using Taqman probe based qPCR for signal quantification.  $\Delta C_t$  is the difference in threshold cycle for the listed concentration of target from a no-target control. Data points for each target represent the average and standard error of two independent assays.

In order to develop the antibody-phage conjugates for multiplexed detection of different cancer biomarkers, two additional antibody-phage conjugates that recognize IL-1 $\beta$  and IL-6 were produced using the photoirradiation techniques used to produce the anti-TNF $\alpha$ -phage. For multiplexed detection, since each antibody-phage needs to encode a DNA sequence that recognizes a specific primer set, we inserted a unique forward primer sequence into the non-coding region of the phage genome for each of the different types of antibody-phage. In order to make sure that there was no erroneous cross-talk between the different primer sets and the different types of antibody-phage, PCR reactions were run from each antibody-phage in the presence of the three different primer sets. As shown in Figure 4.7, only in the presence of the correct primers with the corresponding antibody-phage conjugates (correct phage genome) was any DNA amplification observed.

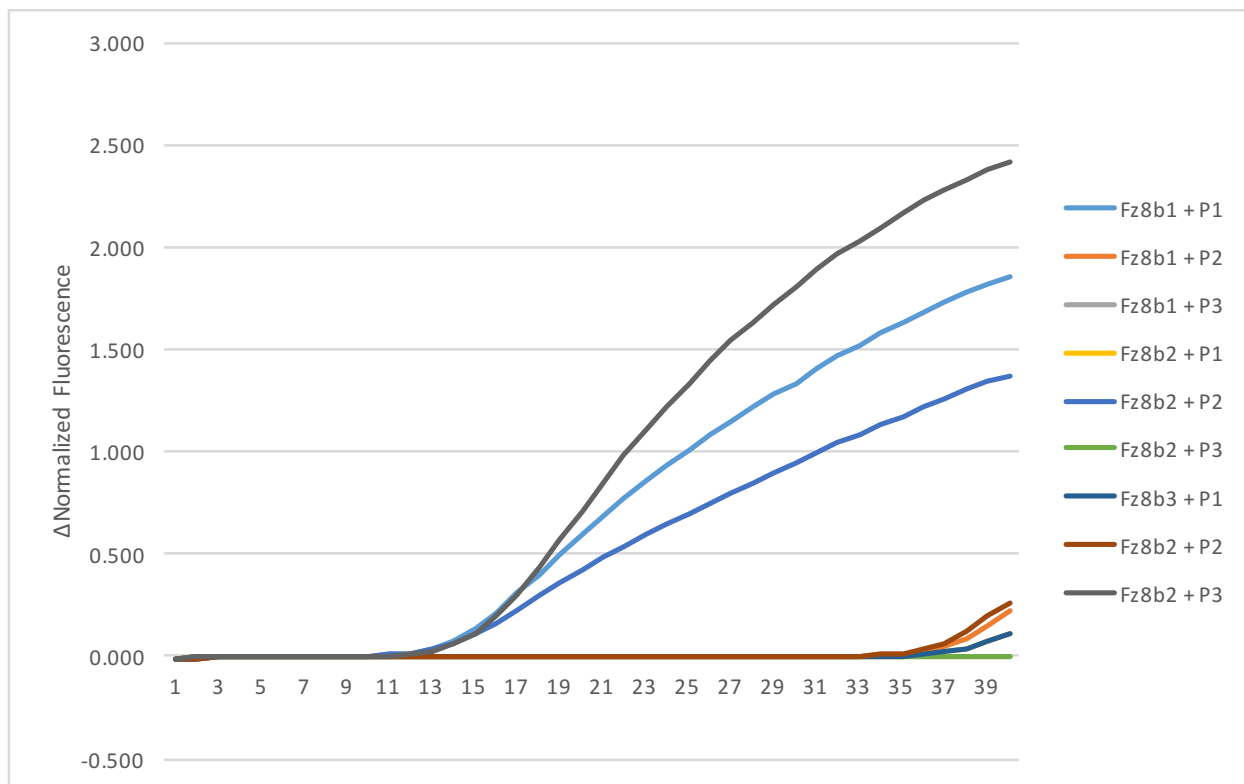


Figure 4.7: Sequence specific real time PCR amplification of various phage via various primers: Taqman probe based real time amplification curves of the three phage types (Fz8b1,2,3) used for multiplex immunoassays diluted to  $1e9/ml$  in reactions with primer sets specific to each phage type (P1,2,3). In multiplex immunoassays, Fz8b1 was conjugated with  $TNF\alpha$ , Fz8b2 with IL6 and Fz8b3 with IL- $1\beta$ .

As had been done with the anti- $TNF\alpha$ -phage, the anti-IL-6-phage and anti-IL- $1\beta$ -phage were tested in real-time PCR assays against different concentrations of IL-6 and IL- $1\beta$  respectively. The  $\Delta C_t$  values for  $TNF\alpha$ , IL-6 and IL- $1\beta$  as a function of antigen concentration are shown in Figure 4.6. As demonstrated, although all of the phage conjugates could detect down to  $10pg/ml$  concentrations, due to the low  $K_D$  for binding between anti-IL6 and IL6, the anti-IL6-phage showed the highest sensitivities which was also corroborated by ELISA. By building such calibration curves for each antibody-phage against each antigen, we could then use the  $\Delta C_t$  values to determine in real time both the type and amount of each antigen in solution.

These studies also showed the limit of detection of each antigen to be below most clinically relevant concentrations.<sup>138,139</sup>

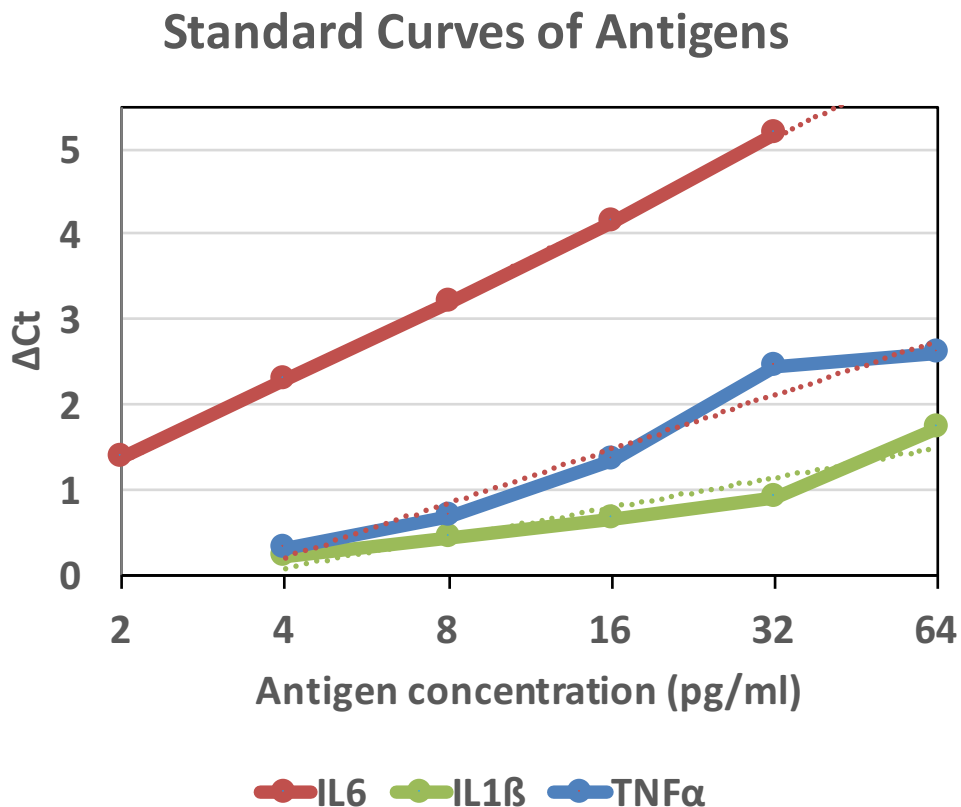


Figure 4.8: Standard curves at low concentrations of three antigens in multiplex assay format: Each antigen listed is diluted to the indicated concentrations and tested in multiplex immunoassay format. Resulting  $\Delta C_t$  values for each dilution series are analyzed for lines of best fit through the least square method. Resulting logarithmic formula are used to calculate the indicated concentration from  $\Delta C_t$  values attained in later multiplex assays testing multiple antigens at once.

Finally, in order to test the antibody-phage conjugates in multiplexed assays, different mixtures of the three antigens (TNF $\alpha$ , IL-6, IL-1 $\beta$ ) were reacted in FBS at concentrations of 10pg/ml with a mixture of beads conjugated with the respective capture antibodies. Next, after removing unbound antigen, the 3 different antibody-phage conjugats were added to the beads in PBST. After incubating for 1 h, unbound antibody-phage conjugates were removed and the

beads were washed 4 times in PBST. The beads were next aliquoted into 3 separate wells to which a Taqman universal mastermix II was added along with the phage specific primers and the universal Taqman probe. Real-time PCR assays were then run as before. Using the resulting  $\Delta C_t$  values and the calibration curves obtained for each target (Figure 4.8), the concentrations within each mixture could be determined (Figure 4.9). While there was some variability in signal such that some of the solutions yielded  $\Delta C_t$  values that correlated to slightly higher than 10 pg/ml antigen, overall the results were consistent and more importantly, in the absence of a particular antigen, no or near negligible signals were obtained. These results therefore show minimal off target effects and demonstrated clear distinctions between all mixtures tested and the potential applicability of these antibody-phage constructs for real time multiplexed immuno-PCR assays.

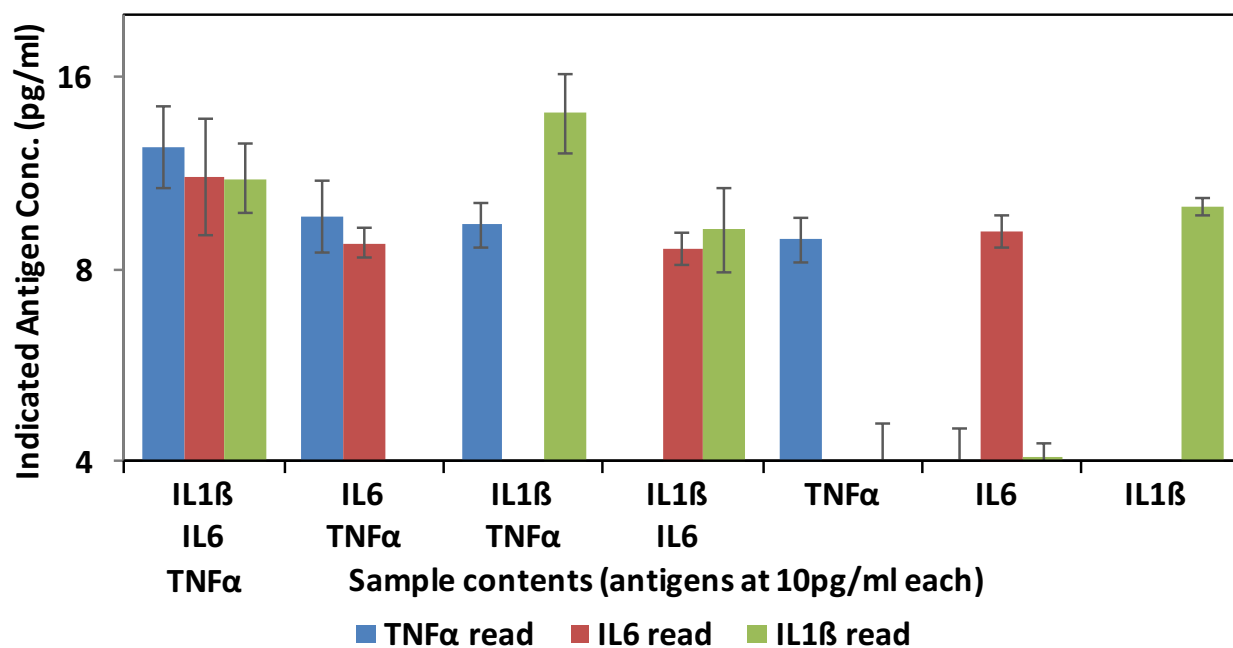


Figure 4.9: Multiplex assay results of various combinations of targets as calculated by the standard curves. Targets listed for each sample are at 10pg/ml. Results are the average and standard error of five independent assays.

#### Section 4.4: Conclusions

We have demonstrated here the novel engineering of covalently-linked antibody-phage constructs in which antibodies can be incorporated without recombinant expression and without affecting their antigen-binding properties. The crosslinked antibody-phage were prevented from binding to any other antibodies in solution or on a surface but can still recognize the specific antigen target. The naturally encased phage genome was utilized as a template for PCR amplification and that encodable domains can be incorporated within the phage DNA that recognize distinct primer sets with high specificity. Furthermore, by utilizing a universal Taqman probe, real-time PCR assays were run with the antibody-phage to build quantitative correlation between a measurable delta Ct value and a specific antigen concentration in solution. Using such calibration curves, a multiplexed assay was developed to detect combinations of TNF $\alpha$ , IL-6, and IL-1 $\beta$  dispersed in a single solution of FBS at concentrations of 10 pg/ml each, which is a low and clinically relevant concentration. Results of the multiplexed assay showed that the antibody-phage both detected and quantified antigens with high sensitivity. Most importantly, in the absence of antigen almost no signal was observed, demonstrating the high specificity of the antibody-phage for a particular antigen. In addition to immuno-PCR, the antibody-phage constructs developed here can also be applied to nanomedicine applications such as targeted drug delivery or *in vivo* imaging contrast agents.<sup>63,114,140,141</sup> Future work will expand the breadth of different antibody-phage conjugates to detect a wider variety of different biomarkers. In addition, we will implement these phage antibodies for biomarker detection in clinical patient samples.

## Chapter 5

### Conclusions and future directions

Throughout this work, I have developed methods of engineering multiple aspects of filamentous bacteriophage for use in protein assays. I have demonstrated how the engineering of phage coat proteins may allow the phage to act as a modular biological scaffold and how this scaffold can be used to enhance the sensitivity of a standard ELISA. Alternatively, the phage genome can be used as a template for DNA amplification reactions including rolling circle amplification and quantitative real-time PCR. These reactions can be used to signal both the amount of phage bound to a protein target as well as the identity of that target. These methods proved particularly useful in combination with antibody-phage conjugates which were shown to bind specifically to their antigens within a multiplex sandwich assay. The sensitivity allowed for the detection of antigens at clinically relevant concentrations and showed the ability to be multiplexed. It is my hope that this assay (or a similar one) will be useful in determining protein concentrations in clinical samples. It may also be improved by combining it with further modification.

For example, a drawback to the use of phage in protein sensing assays has been their propensity to bind non-specifically to many assay surfaces. Though the large surface area of the phage particles was used to the advantage of the enhanced ELISA discussed in Chapter 2, it also is likely causing phage particles to bind non-covalently via non-specific charge-charge interactions assay surfaces. This, in turn, has caused relatively large background signals as opposed to traditional assays using conjugated antibodies. I believe this effect could be alleviated in two ways, on which I have done preliminary work.

First, it has been shown previously that zwitterionic peptides can be used to block non-specific binding by forming a hydration layer.<sup>142</sup> I have attempted to use this effect to create phage that are less likely to bind non-specifically by expressing short zwitterionic sequences on the solvent exposed N-terminus of their p8 major coat protein. The N-terminus of the p8 protein contains several negatively charged glutamic and aspartic acid residues which counteract the lysine residues present at the C-terminus to form a dipolar protein. Because this dipolar nature is thought to be crucial for the proper assembly of the bacteriophage capsid, it was unclear how amenable the phage would be to the insertion of positive residue within the N-terminus.<sup>62</sup> However, after modifying the p8 coat protein sequence of an Fd-tet type phage from N-AEGE to N-AEKEKE it was found that the modified phage expressed the modified p8 well. If this modification could be combined with a targeted phage, such as the photo-crosslinked antibody-phage, it may allow for increased sensitivity when using that phage in immunoassays.

Second, I have also attempted to simply lower the amount of surface area per phage particle by shortening overall length of the phage. I attempted this with the antibody photocrosslinking phage by switching their expression to a phagemid type system. In this system I expressed their modified phage coat proteins from a helper plasmid, which packaged a small piece of phagemid DNA rather than the large phage genome.<sup>22</sup> Because the length of the phage capsids is determined by the length of the DNA that is packaged in them, the phage that were produced from this expression system were significantly shorter (approximately 350nm rather than 1300nm). This was verified by transmission electron microscopy. However, because the phage needed to be produced in a strain also carrying a plasmid containing the machinery for BPA incorporation, the expression proved difficult, with the titers of phage produced frequently being much lower than normal. Even so, I think it is likely that the expression system could be

optimized to produce short antibody photocrosslinking phage. It is my hope that one or a combination of these approaches could be used to further increase the sensitivity of assays using phage.

The strategies for phage modification developed in this work will be of use in applications outside of protein sensing. These include phage therapy, where phage are used to infect pathogenic bacterium within a patient, or applications of phage in-vivo such as imaging, gene or drug delivery.

Since their discovery, bacteriophage have captured the interest of scientists and engineers alike by their comparative simplicity in a complex biological surrounding. A hundred and one years of focused research with them has yielded a comprehensive understanding of their function and modification that is matched by few other biological systems. This research has yielded many of the most important discoveries of molecular biology and some of its most powerful methods. The work discussed here adds to that legacy and demonstrates that phage continue to hold promising solutions to the great engineering challenges of today.

## Bibliography

1. Salmond, G. P. C. & Fineran, P. C. A century of the phage: past, present and future. *Nat. Rev. Microbiol.* **13**, 777–786 (2015).
2. Twort, F. W. Originally published as Volume 2, Issue 4814AN INVESTIGATION ON THE NATURE OF ULTRA-MICROSCOPIC VIRUSES. *The Lancet* **186**, 1241–1243 (1915).
3. Duckworth, D. H. ‘Who discovered bacteriophage?’. *Bacteriol. Rev.* **40**, 793–802 (1976).
4. On an invisible microbe antagonistic to dysentery bacilli. Note by M. F. d’Herelle, presented by M. Roux. *Comptes Rendus Academie des Sciences* 1917; 165:373–5. *Bacteriophage* **1**, 3–5 (2011).
5. Luria, S. E. & Delbrück, M. Mutations of Bacteria from Virus Sensitivity to Virus Resistance. *Genetics* **28**, 491–511 (1943).
6. Luria, S. E. Reactivation of Irradiated Bacteriophage by Transfer of Self-Reproducing Units. *Proc. Natl. Acad. Sci. U. S. A.* **33**, 253–264 (1947).
7. Hershey, A. D. & Chase, M. Independent functions of viral protein and nucleic acid in growth of bacteriophage. *J. Gen. Physiol.* **36**, 39–56 (1952).
8. Dulbecco, R. Production of Plaques in Monolayer Tissue Cultures by Single Particles of an Animal Virus. *Proc. Natl. Acad. Sci. U. S. A.* **38**, 747–752 (1952).
9. Demerec, M. & Fano, U. Bacteriophage-Resistant Mutants in Escherichia Coli. *Genetics* **30**, 119–136 (1945).
10. Hofschneider, P. H. & Preuss, A. M 13 bacteriophage liberation from intact bacteria as revealed by electron microscopy. *J. Mol. Biol.* **7**, 450–IN5 (1963).

11. Marvin, D. A. & Hoffmann-Berling, H. Physical and Chemical Properties of Two New Small Bacteriophages. *Nature* **197**, (1963).
12. van Wezenbeek, P. M., Hulsebos, T. J. & Schoenmakers, J. G. Nucleotide sequence of the filamentous bacteriophage M13 DNA genome: comparison with phage fd. *Gene* **11**, 129–148 (1980).
13. *Phage Display: A Laboratory Manual*. (CSHL Press, 2004).
14. Zinder, N. D. & Boeke, J. D. The filamentous phage (Ff) as vectors for recombinant DNA--a review. *Gene* **19**, 1–10 (1982).
15. Smith, G. P. Filamentous fusion phage: novel expression vectors that display cloned antigens on the virion surface. *Science* **228**, 1315–1317 (1985).
16. Parmley, S. F. & Smith, G. P. Antibody-selectable filamentous fd phage vectors: affinity purification of target genes. *Gene* **73**, 305–318 (1988).
17. Smith, G. P. & Petrenko, V. A. Phage Display. *Chem. Rev.* **97**, 391–410 (1997).
18. Katz, B. A. Binding to protein targets of peptidic leads discovered by phage display: crystal structures of streptavidin-bound linear and cyclic peptide ligands containing the HPQ sequence. *Biochemistry (Mosc.)* **34**, 15421–15429 (1995).
19. McCafferty, J., Griffiths, A. D., Winter, G. & Chiswell, D. J. Phage antibodies: filamentous phage displaying antibody variable domains. *Nature* **348**, 552–554 (1990).
20. Hoogenboom, H. R. *et al.* Multi-subunit proteins on the surface of filamentous phage: methodologies for displaying antibody (Fab) heavy and light chains. *Nucleic Acids Res.* **19**, 4133–4137 (1991).
21. Marks, J. D. *et al.* By-passing immunization. *J. Mol. Biol.* **222**, 581–597 (1991).

22. Chasteen, L., Ayriss, J., Pavlik, P. & Bradbury, A. R. M. Eliminating helper phage from phage display. *Nucleic Acids Res.* **34**, e145–e145 (2006).
23. Soltes, G. *et al.* A new helper phage and phagemid vector system improves viral display of antibody Fab fragments and avoids propagation of insert-less virions. *J. Immunol. Methods* **274**, 233–244 (2003).
24. Petrenko, V. A. & Smith, G. P. Phages from landscape libraries as substitute antibodies. *Protein Eng.* **13**, 589–592 (2000).
25. Zhong, G., Smith, G. P., Berry, J. & Brunham, R. C. Conformational mimicry of a chlamydial neutralization epitope on filamentous phage. *J. Biol. Chem.* **269**, 24183–24188 (1994).
26. Enshell-Seijffers, D., Smelyanski, L. & Gershoni, J. M. The rational design of a ‘type 88’ genetically stable peptide display vector in the filamentous bacteriophage fd. *Nucleic Acids Res.* **29**, e50 (2001).
27. Gao, C. *et al.* A method for the generation of combinatorial antibody libraries using pIX phage display. *Proc. Natl. Acad. Sci. U. S. A.* **99**, 12612–12616 (2002).
28. Huovinen, T. *et al.* The selection performance of an antibody library displayed on filamentous phage coat proteins p9, p3 and truncated p3. *BMC Res. Notes* **7**, 661 (2014).
29. Ghosh, D., Kohli, A. G., Moser, F., Endy, D. & Belcher, A. M. Refactored M13 Bacteriophage as a Platform for Tumor Cell Imaging and Drug Delivery. *ACS Synth. Biol.* **1**, 576–582 (2012).
30. Fernandez-Gacio, A., Uguen, M. & Fastrez, J. Phage display as a tool for the directed evolution of enzymes. *Trends Biotechnol.* **21**, 408–414 (2003).

31. Pasqualini, R. & Ruoslahti, E. Organ targeting In vivo using phage display peptide libraries. *Nature* **380**, 364–366 (1996).
32. Hart, S. L. *et al.* Cell binding and internalization by filamentous phage displaying a cyclic Arg-Gly-Asp-containing peptide. *J. Biol. Chem.* **269**, 12468–12474 (1994).
33. Rangel, R. *et al.* Targeting mammalian organelles with internalizing phage (iPhage) libraries. *Nat. Protoc.* **8**, 1916–1939 (2013).
34. Van Dorst, B., Mehta, J., Rouah-Martin, E., Blust, R. & Robbens, J. Phage display as a method for discovering cellular targets of small molecules. *Methods* **58**, 56–61 (2012).
35. Kim, H.-Y., Wang, X., Wahlberg, B. & Edwards, W. B. Discovery of Hapten-Specific scFv from a Phage Display Library and Applications for HER2-Positive Tumor Imaging. *Bioconjug. Chem.* **25**, 1311–1322 (2014).
36. Zhang, X., Zhang, C., Liu, Y., Yu, X. & Liu, X. Construction of scFv phage display library with hapten-specific repertoires and characterization of anti-ivermectin fragment isolated from the library. *Eur. Food Res. Technol.* **231**, 423–430 (2010).
37. Seker, U. O. S. & Demir, H. V. Material Binding Peptides for Nanotechnology. *Molecules* **16**, 1426–1451 (2011).
38. Care, A., Bergquist, P. L. & Sunna, A. Solid-binding peptides: smart tools for nanobiotechnology. *Trends Biotechnol.* **33**, 259–268 (2015).
39. Sunna, A., Chi, F. & Bergquist, P. L. A linker peptide with high affinity towards silica-containing materials. *New Biotechnol.* **30**, 485–492 (2013).
40. Kacar, T. *et al.* Directed self-immobilization of alkaline phosphatase on micro-patterned substrates via genetically fused metal-binding peptide. *Biotechnol. Bioeng.* **103**, 696–705 (2009).

41. Naik, R. R., Stringer, S. J., Agarwal, G., Jones, S. E. & Stone, M. O. Biomimetic synthesis and patterning of silver nanoparticles. *Nat. Mater.* **1**, 169–172 (2002).
42. Chiu, C.-Y. *et al.* Platinum nanocrystals selectively shaped using facet-specific peptide sequences. *Nat. Chem.* **3**, 393–399 (2011).
43. Palafox-Hernandez, J. P. *et al.* Comparative Study of Materials-Binding Peptide Interactions with Gold and Silver Surfaces and Nanostructures: A Thermodynamic Basis for Biological Selectivity of Inorganic Materials. *Chem. Mater.* **26**, 4960–4969 (2014).
44. Bar, H., Yacoby, I. & Benhar, I. Killing cancer cells by targeted drug-carrying phage nanomedicines. *BMC Biotechnol.* **8**, 37 (2008).
45. Newton, J. R., Miao, Y., Deutscher, S. L. & Quinn, T. P. Melanoma Imaging with Pretargeted Bivalent Bacteriophage. *J. Nucl. Med.* **48**, 429–436 (2007).
46. Rusckowski, M., Gupta, S., Liu, G., Dou, S. & Hnatowich, D. J. Investigation of four (99m)Tc-labeled bacteriophages for infection-specific imaging. *Nucl. Med. Biol.* **35**, 433–440 (2008).
47. Li, K. *et al.* Chemical Modification of M13 Bacteriophage and Its Application in Cancer Cell Imaging. *Bioconjug. Chem.* **21**, 1369–1377 (2010).
48. Yi, H. *et al.* M13 Phage-Functionalized Single-Walled Carbon Nanotubes As Nanoprobes for Second Near-Infrared Window Fluorescence Imaging of Targeted Tumors. *Nano Lett.* **12**, 1176–1183 (2012).
49. Stevens, T. K. *et al.* HyperCEST detection of a <sup>129</sup>Xe-based contrast agent composed of cryptophane-A molecular cages on a bacteriophage scaffold. *Magn. Reson. Med.* **69**, 1245–1252 (2013).

50. Ghosh, D. *et al.* M13-templated magnetic nanoparticles for targeted in vivo imaging of prostate cancer. *Nat. Nanotechnol.* **7**, 677–682 (2012).
51. Ghosh, D. *et al.* Deep, noninvasive imaging and surgical guidance of submillimeter tumors using targeted M13-stabilized single-walled carbon nanotubes. *Proc. Natl. Acad. Sci. U. S. A.* **111**, 13948–13953 (2014).
52. Palaniappan, K. K. *et al.* Molecular Imaging of Cancer Cells Using a Bacteriophage-Based <sup>129</sup>Xe NMR Biosensor. *Angew. Chem. Int. Ed.* **52**, 4849–4853 (2013).
53. Jin, H.-E., Farr, R. & Lee, S.-W. Collagen mimetic peptide engineered M13 bacteriophage for collagen targeting and imaging in cancer. *Biomaterials* **35**, 9236–9245 (2014).
54. Larocca, D., Jensen-Pergakes, K., Burg, M. A. & Baird, A. Receptor-Targeted Gene Delivery Using Multivalent Phagemid Particles. *Mol. Ther.* **3**, 476–484 (2001).
55. Larocca, D. *et al.* Evolving phage vectors for cell targeted gene delivery. *Curr. Pharm. Biotechnol.* **3**, 45–57 (2002).
56. Yoo, S. Y. *et al.* M13 Bacteriophage and Adeno-Associated Virus Hybrid for Novel Tissue Engineering Material with Gene Delivery Functions. *Adv. Healthc. Mater.* **5**, 88–93 (2016).
57. Baird, A. Gene Transfer into Mammalian Cells Using Targeted Filamentous Bacteriophage. *Cold Spring Harb. Protoc.* **2011**, pdb.prot5653 (2011).
58. Bakhshinejad, B. & Sadeghizadeh, M. Bacteriophages as vehicles for gene delivery into mammalian cells: prospects and problems. *Expert Opin. Drug Deliv.* **11**, 1561–1574 (2014).
59. Loc-Carrillo, C. & Abedon, S. T. Pros and cons of phage therapy. *Bacteriophage* **1**, 111–114 (2011).
60. Skurnik, M. & Strauch, E. Phage therapy: Facts and fiction. *Int. J. Med. Microbiol.* **296**, 5–14 (2006).

61. Lee, Y. J. *et al.* Fabricating Genetically Engineered High-Power Lithium-Ion Batteries Using Multiple Virus Genes. *Science* **324**, 1051–1055 (2009).
62. Lee, B. Y. *et al.* Virus-based piezoelectric energy generation. *Nat. Nanotechnol.* **7**, 351–356 (2012).
63. Lee, J. H. & Cha, J. N. Amplified Protein Detection through Visible Plasmon Shifts in Gold Nanocrystal Solutions from Bacteriophage Platforms. *Anal. Chem.* **83**, 3516–3519 (2011).
64. Lee, J. H., Domaille, D. W. & Cha, J. N. Amplified Protein Detection and Identification through DNA-Conjugated M13 Bacteriophage. *ACS Nano* **6**, 5621–5626 (2012).
65. Domaille, D. W., Lee, J. H. & Cha, J. N. High density DNA loading on the M13 bacteriophage provides access to colorimetric and fluorescent protein microarray biosensors. *Chem. Commun.* **49**, 1759 (2013).
66. Lee, J. H. *et al.* M13 Bacteriophage as Materials for Amplified Surface Enhanced Raman Scattering Protein Sensing. *Adv. Funct. Mater.* **24**, 2079–2084 (2014).
67. Mousa, S. Biosensors: the new wave in cancer diagnosis. *Nanotechnol. Sci. Appl.* **1** (2010). doi:10.2147/NSA.S13465
68. Brambilla, D. *et al.* Nanotechnologies for Alzheimer's disease: diagnosis, therapy, and safety issues. *Nanomedicine Nanotechnol. Biol. Med.* **7**, 521–540 (2011).
69. Ferrari, M. Cancer nanotechnology: opportunities and challenges. *Nat. Rev. Cancer* **5**, 161–171 (2005).
70. Borisov, S. M. & Wolfbeis, O. S. Optical Biosensors. *Chem. Rev.* **108**, 423–461 (2008).
71. Kim, D., Daniel, W. L. & Mirkin, C. A. Microarray-Based Multiplexed Scanometric Immunoassay for Protein Cancer Markers Using Gold Nanoparticle Probes. *Anal. Chem.* **81**, 9183–9187 (2009).

72. Stoeva, S. I., Lee, J.-S., Smith, J. E., Rosen, S. T. & Mirkin, C. A. Multiplexed Detection of Protein Cancer Markers with Biobarcoded Nanoparticle Probes. *J. Am. Chem. Soc.* **128**, 8378–8379 (2006).
73. Ke, R., Yang, W., Xia, X., Xu, Y. & Li, Q. Tandem conjugation of enzyme and antibody on silica nanoparticle for enzyme immunoassay. *Anal. Biochem.* **406**, 8–13 (2010).
74. Dhawan, S. Design and construction of novel molecular conjugates for signal amplification (I): conjugation of multiple horseradish peroxidase molecules to immunoglobulin via primary amines on lysine peptide chains. *Peptides* **23**, 2091–2098 (2002).
75. Dhawan, S. Design and construction of novel molecular conjugates for signal amplification (II): use of multivalent polystyrene microparticles and lysine peptide chains to generate immunoglobulin–horseradish peroxidase conjugates. *Peptides* **23**, 2099–2110 (2002).
76. Oh, J.-W. *et al.* Biomimetic virus-based colourimetric sensors. *Nat. Commun.* **5**, (2014).
77. Jin, H. *et al.* Quantum dot-engineered M13 virus layer-by-layer composite films for highly selective and sensitive turn-on TNT sensors. *Chem. Commun.* **49**, 6045–6047 (2013).
78. Lakshmanan, R. S. *et al.* Detection of Salmonella typhimurium in fat free milk using a phage immobilized magnetoelastic sensor. *Sens. Actuators B Chem.* **126**, 544–550 (2007).
79. Pacheco-Gómez, R. *et al.* Detection of Pathogenic Bacteria Using a Homogeneous Immunoassay Based on Shear Alignment of Virus Particles and Linear Dichroism. *Anal. Chem.* **84**, 91–97 (2012).
80. Mao, C. *et al.* Virus-Based Toolkit for the Directed Synthesis of Magnetic and Semiconducting Nanowires. *Science* **303**, 213–217 (2004).
81. Courchesne, N.-M. D. *et al.* Assembly of a Bacteriophage-Based Template for the Organization of Materials into Nanoporous Networks. *Adv. Mater.* **26**, 3398–3404 (2014).

82. Gandra, N., Wang, D.-D., Zhu, Y. & Mao, C. Virus-Mimetic Cytoplasm-Cleavable Magnetic/Silica Nanoclusters for Enhanced Gene Delivery to Mesenchymal Stem Cells. *Angew. Chem. Int. Ed.* **52**, 11278–11281 (2013).
83. Suthiwangcharoen, N. *et al.* M13 bacteriophage-polymer nanoassemblies as drug delivery vehicles. *Nano Res.* **4**, 483–493 (2011).
84. Petrenko, V. A., Smith, G. P., Gong, X. & Quinn, T. A library of organic landscapes on filamentous phage. *Protein Eng.* **9**, 797–801 (1996).
85. Scott, J. K. & Smith, G. P. Searching for peptide ligands with an epitope library. *Science* **249**, 386–390 (1990).
86. Clackson, T., Hoogenboom, H. R., Griffiths, A. D. & Winter, G. Making antibody fragments using phage display libraries. *Nature* **352**, 624–628 (1991).
87. Yacoby, I., Shamis, M., Bar, H., Shabat, D. & Benhar, I. Targeting Antibacterial Agents by Using Drug-Carrying Filamentous Bacteriophages. *Antimicrob. Agents Chemother.* **50**, 2087–2097 (2006).
88. Nilsson, B. *et al.* A synthetic IgG-binding domain based on staphylococcal protein A. *Protein Eng.* **1**, 107–113 (1987).
89. Lee, S.-K., Yun, D. S. & Belcher, A. M. Cobalt Ion Mediated Self-Assembly of Genetically Engineered Bacteriophage for Biomimetic Co–Pt Hybrid Material. *Biomacromolecules* **7**, 14–17 (2006).
90. Nam, K. T. *et al.* Virus-Enabled Synthesis and Assembly of Nanowires for Lithium Ion Battery Electrodes. *Science* **312**, 885–888 (2006).
91. Noren, K. A. & Noren, C. J. Construction of High-Complexity Combinatorial Phage Display Peptide Libraries. *Methods* **23**, 169–178 (2001).

92. Carrico, Z. M. *et al.* N-Terminal Labeling of Filamentous Phage To Create Cancer Marker Imaging Agents. *ACS Nano* **6**, 6675–6680 (2012).
93. Witus, L. S. *et al.* Identification of highly reactive sequences for PLP-mediated bioconjugation using a combinatorial peptide library. *J. Am. Chem. Soc.* **132**, 16812–16817 (2010).
94. Scheck, R. A., Dedeo, M. T., Iavarone, A. T. & Francis, M. B. Optimization of a Biomimetic Transamination Reaction. *J. Am. Chem. Soc.* **130**, 11762–11770 (2008).
95. Uludag, Y. & Tothill, I. E. Cancer Biomarker Detection in Serum Samples Using Surface Plasmon Resonance and Quartz Crystal Microbalance Sensors with Nanoparticle Signal Amplification. *Anal. Chem.* **84**, 5898–5904 (2012).
96. Katsamba, P. S. *et al.* Kinetic analysis of a high-affinity antibody/antigen interaction performed by multiple Biacore users. *Anal. Biochem.* **352**, 208–221 (2006).
97. Karlsson, R. & Fält, A. Experimental design for kinetic analysis of protein-protein interactions with surface plasmon resonance biosensors. *J. Immunol. Methods* **200**, 121–133 (1997).
98. O'Connell, D., Becerril, B., Roy-Burman, A., Daws, M. & Marks, J. D. Phage versus Phagemid Libraries for Generation of Human Monoclonal Antibodies. *J. Mol. Biol.* **321**, 49–56 (2002).
99. Poul, M. A., Becerril, B., Nielsen, U. B., Morisson, P. & Marks, J. D. Selection of tumor-specific internalizing human antibodies from phage libraries. *J. Mol. Biol.* **301**, 1149–1161 (2000).
100. Yoo, S. Y., Merzlyak, A. & Lee, S.-W. Facile growth factor immobilization platform based on engineered phage matrices. *Soft Matter* **7**, 1660 (2011).

101. Weber, P. C., Pantoliano, M. W. & Thompson, L. D. Crystal structure and ligand binding studies of a screened peptide complexed with streptavidin. *Biochemistry (Mosc.)* **31**, 9350–9354 (1992).
102. Sano, T., Smith, C. L. & Cantor, C. R. Immuno-PCR: very sensitive antigen detection by means of specific antibody-DNA conjugates. *Science* **258**, 120–122 (1992).
103. Kazane, S. A. *et al.* Site-specific DNA-antibody conjugates for specific and sensitive immuno-PCR. *Proc. Natl. Acad. Sci.* **109**, 3731–3736 (2012).
104. Burbulis, I., Yamaguchi, K., Gordon, A., Carlson, R. & Brent, R. Using protein-DNA chimeras to detect and count small numbers of molecules. *Nat. Methods* **2**, 31–37 (2005).
105. Niemeyer, C. M., Adler, M. & Wacker, R. Immuno-PCR: high sensitivity detection of proteins by nucleic acid amplification. *Trends Biotechnol.* **23**, 208–216 (2005).
106. Joerger, R. D., Truby, T. M., Hendrickson, E. R., Young, R. M. & Ebersole, R. C. Analyte detection with DNA-labeled antibodies and polymerase chain reaction. *Clin. Chem.* **41**, 1371–1377 (1995).
107. Flanigan, J. *et al.* Multiplex protein detection with DNA readout via mass spectrometry. *New Biotechnol.* **30**, 153–158 (2013).
108. Schweitzer, B. *et al.* Immunoassays with rolling circle DNA amplification: A versatile platform for ultrasensitive antigen detection. *Proc. Natl. Acad. Sci.* **97**, 10113–10119 (2000).
109. Schweitzer, B. *et al.* Multiplexed protein profiling on microarrays by rolling-circle amplification. *Nat. Biotechnol.* **20**, 359–365 (2002).
110. Lee, J.-W., Song, J., Hwang, M. P. & Lee, K. H. Nanoscale bacteriophage biosensors beyond phage display. *Int. J. Nanomedicine* **8**, 3917–3925 (2013).

111. Chen, L., Zhao, X., Lin, Y., Su, Z. & Wang, Q. Dual stimuli-responsive supramolecular hydrogel of bionanoparticles and hyaluronan. *Polym. Chem.* **5**, 6754–6760 (2014).
112. Bernard, J. M. L. & Francis, M. B. Chemical strategies for the covalent modification of filamentous phage. *Front. Microbiol.* **5**, 734 (2014).
113. Brasino, M., Lee, J. H. & Cha, J. N. Creating highly amplified enzyme-linked immunosorbent assay signals from genetically engineered bacteriophage. *Anal. Biochem.* doi:10.1016/j.ab.2014.10.006
114. Guo, Y.-C. *et al.* Phage display mediated immuno-PCR. *Nucleic Acids Res.* **34**, e62 (2006).
115. Takahashi, H., Yamamoto, K., Ohtani, T. & Sugiyama, S. Cell-free cloning using multiply-primed rolling circle amplification with modified RNA primers. *BioTechniques* **47**, 609–615 (2009).
116. Hutchison, C. A., Smith, H. O., Pfannkoch, C. & Venter, J. C. Cell-free cloning using  $\phi$ 29 DNA polymerase. *Proc. Natl. Acad. Sci. U. S. A.* **102**, 17332–17336 (2005).
117. Srila, W. & Yamabhai, M. Identification of Amino Acid Residues Responsible for the Binding to Anti-FLAG<sup>TM</sup> M2 Antibody Using a Phage Display Combinatorial Peptide Library. *Appl. Biochem. Biotechnol.* **171**, 583–589 (2013).
118. Miceli, R. M., DeGraaf, M. E. & Fischer, H. D. Two-stage selection of sequences from a random phage display library delineates both core residues and permitted structural range within an epitope. *J. Immunol. Methods* **167**, 279–287 (1994).
119. Dean, F. B., Nelson, J. R., Giesler, T. L. & Lasken, R. S. Rapid Amplification of Plasmid and Phage DNA Using Phi29 DNA Polymerase and Multiply-Primed Rolling Circle Amplification. *Genome Res.* **11**, 1095–1099 (2001).

120. Nallur, G. *et al.* Signal amplification by rolling circle amplification on DNA microarrays. *Nucleic Acids Res.* **29**, e118 (2001).
121. Dean, F. B. *et al.* Comprehensive human genome amplification using multiple displacement amplification. *Proc. Natl. Acad. Sci. U. S. A.* **99**, 5261–5266 (2002).
122. Madan, B., Chaudhary, G., Cramer, S. M. & Chen, W. ELP-z and ELP-zz capturing scaffolds for the purification of immunoglobulins by affinity precipitation. *J. Biotechnol.* **163**, 10–16 (2013).
123. Konrad, A., Eriksson Karlström, A. & Hober, S. Covalent Immunoglobulin Labeling through a Photoactivable Synthetic Z Domain. *Bioconjug. Chem.* **22**, 2395–2403 (2011).
124. Wegner, G. J., Lee, H. J. & Corn, R. M. Characterization and Optimization of Peptide Arrays for the Study of Epitope–Antibody Interactions Using Surface Plasmon Resonance Imaging. *Anal. Chem.* **74**, 5161–5168 (2002).
125. Hilpert, K. *et al.* Anti-c-myc antibody 9E10: epitope key positions and variability characterized using peptide spot synthesis on cellulose. *Protein Eng.* **14**, 803–806 (2001).
126. Hui, J. Z. & Tsourkas, A. Optimization of Photoactive Protein Z for Fast and Efficient Site-Specific Conjugation of Native IgG. *Bioconjug. Chem.* **25**, 1709–1719 (2014).
127. Liu, C. C. *et al.* Protein evolution with an expanded genetic code. *Proc. Natl. Acad. Sci.* **105**, 17688–17693 (2008).
128. Rusling, J. F., Kumar, C. V., Gutkind, J. S. & Patel, V. Measurement of biomarker proteins for point-of-care early detection and monitoring of cancer. *The Analyst* **135**, 2496–2511 (2010).
129. Hanash, S. M. Why have protein biomarkers not reached the clinic? *Genome Med.* **3**, 66 (2011).

130. Rifai, N., Gillette, M. A. & Carr, S. A. Protein biomarker discovery and validation: the long and uncertain path to clinical utility. *Nat. Biotechnol.* **24**, 971–983 (2006).
131. Hendrickson, E. R., Truby, T. M., Joerger, R. D., Majarian, W. R. & Ebersole, R. C. High sensitivity multianalyte immunoassay using covalent DNA-labeled antibodies and polymerase chain reaction. *Nucleic Acids Res.* **23**, 522–529 (1995).
132. Frenzel, A., Hust, M. & Schirrmann, T. Expression of Recombinant Antibodies. *Front. Immunol.* **4**, (2013).
133. Tamkovich, S. N. *et al.* Circulating DNA and DNase activity in human blood. *Ann. N. Y. Acad. Sci.* **1075**, 191–196 (2006).
134. Chin, J. W., Martin, A. B., King, D. S., Wang, L. & Schultz, P. G. Addition of a photocrosslinking amino acid to the genetic code of Escherichia coli. *Proc. Natl. Acad. Sci.* **99**, 11020–11024 (2002).
135. Young, T. S., Ahmad, I., Yin, J. A. & Schultz, P. G. An enhanced system for unnatural amino acid mutagenesis in E. coli. *J. Mol. Biol.* **395**, 361–374 (2010).
136. Brasino, M. D. & Cha, J. N. Isothermal rolling circle amplification of virus genomes for rapid antigen detection and typing. *Analyst* **140**, 5138–5144 (2015).
137. Deisenhofer, J. Crystallographic refinement and atomic models of a human Fc fragment and its complex with fragment B of protein A from Staphylococcus aureus at 2.9- and 2.8-Å resolution. *Biochemistry (Mosc.)* **20**, 2361–2370 (1981).
138. Kleiner, G. *et al.* Cytokine Levels in the Serum of Healthy Subjects, Cytokine Levels in the Serum of Healthy Subjects. *Mediat. Inflamm. Mediat. Inflamm.* **2013**, **2013**, e434010 (2013).
139. Yurkovetsky, Z. R. *et al.* Multiplex Analysis of Serum Cytokines in Melanoma Patients Treated with Interferon- $\alpha$ 2b. *Clin. Cancer Res.* **13**, 2422–2428 (2007).

140. Lobo, D. P. *et al.* Direct detection and measurement of wall shear stress using a filamentous bio-nanoparticle. *Nano Res.* **8**, 3307–3315 (2015).
141. Zhang, H. *et al.* Natural phage nanoparticle-mediated real-time immuno-PCR for ultrasensitive detection of protein marker. *Chem. Commun.* **49**, 3778–3780 (2013).
142. Nowinski, A. K., White, A. D., Keefe, A. J. & Jiang, S. Biologically Inspired Stealth Peptide-Capped Gold Nanoparticles. *Langmuir* **30**, 1864–1870 (2014).